Introduction to μSR
Muon Spin Rotation/Relaxation

Elvezio Morenzoni

Paul Scherrer Institute

- The polarized muon as a magnetic micro-probe
- Generation of polarized muon beams
- Time evolution of muon spin polarization: depolarization and relaxation
- Some typical examples
- Magnetism
- Superconductivity
- Studies in thin films, heterostructures
- Not treated: many things: Muonium (semiconductors), level crossing techniques (chemistry, soft matter), dynamical and critical phenomena (magnetism), resonance…

http://people.web.psi.ch/morenzoni

Script of lecture ETH-Z/Uni ZH: Physics with muons

Literature

BOOKS

•A. Yaouanc, P. Dalmas de Réotier, MUON SPIN ROTATION, RELAXATION and RESONANCE (Oxford University Press, 2010)

•A. Schenck, MUON SPIN ROTATION SPECTROSCOPY, (Adam Hilger, Bristol 1985)

•E. Karlsson, SOLID STATE PHENOMENA, As Seen by Muons, Protons, and Excited Nuclei, (Clarendon, Oxford 1995)

•S.L. Lee, S.H. Kilcoyne, R. Cywinski eds, MUON SCIENCE: MUONS IN PHYSICS; CHEMISTRY AND MATERIALS, (IOP Publishing, Bristol and Philadelphia, 1999)

•INTRODUCTORY ARTICLES

•S.J. Blundell, SPIN-POLARIZED MUONS IN CONDENSED MATTER PHYSICS, Contemporary Physics 40, 175 (1999)

•P. Bakule, E. Morenzoni, GENERATION AND APPLICATIONN OF SLOW POLARIZED MUONS, Contemporary Physics 45, 203-225 (2004).

REVIEW ARTICLES, APPLICATIONS

•P. Dalmas de Réotier and A. Yaouanc, MUON SPIN ROTATION AND RELAXATION IN MAGNETIC MATERIALS, J. Phys. Condens. Matter 9 (1997) pp. 9113-9166

•A. Schenck and F.N. Gygax, MAGNETIC MATERIALS STUDIED BY MUON SPIN ROTATION SPECTROSCOPY, In: Handbook of Magnetic Materials, edited by K.H.J. Buschow, Vol. 9 (Elsevier, Amsterdam 1995) pp. 57-302

•B.D. Patterson, MUONIUM STATES IN SEMICONDUCTORS, Rev. Mod. Phys. 60 (1988) pp. 69-159

•A. Amato, HEAVY-FERMION SYSTEMS STUDIED BY μSR TECHNIQUES, Rev. Mod. Phys., 69, 1119 (1997)

•V. Storchak, N. Prokovev, QUANTUM DIFFUSION OF MUONS AND MUONIUM ATOMS IN SOLIDS, Rev. Mod. Physics, 70, 929 (1998)

•J. Sonier, J. Brewer, R. Kiefl, μSR STUDIES OF VORTEX STATE IN TYPE-II SUPERCONDUCTORS, Rev. Mod. Physics, 72, 769 (2000)

•E. Roduner, THE POSITIVE MUON AS A PROBE IN FREE RADICAL CHEMISTRY, Lecture Notes in Chemistry No. 49 (Springer Verlag, Berlin 1988)

Muon properties

Properties of polarized (positive) muons make them sensitive magnetic microprobes of matter.

Mass:	$m_\mu = 105.658\ \mathrm{MeV/c^2} \approx 207\ m_e \approx 1/9\ m_p$	
Charge:	**+e, (-e)**	**interstitial position (generally), local probe**
Spin :	**s= ½**	
Magnetic moment:	$\mu_\mu = g_\mu \frac{e\hbar}{2m_\mu} s$	$(g_\mu \cong 2.\ 001165\ 920\ 69\ (60))$
	$\mu_\mu = 3.18\ \mu_p$	**very sensitive magnetic probe** 10^{-3} **-** $10^{-4}\ \mu_B$ **(no quadrupolar effects)**
Gyromagnetic ratio:	$\gamma_\mu = \frac{\mu_\mu}{\hbar s} = g_\mu \frac{e}{2m_\mu}$	**851.615 MHz/T**
Life time:	$\tau_\mu = 2.19714\ \mu s$	**Fluctuation time window** $10^{-5} < t < 10^{-11}$ **s**
Bound state:	$\mu^+ e^-$	**Muonium, H-Isotop**

μSR: Muon Spin Rotation/Relaxation

Method:

▪Implant and thermalize ~100% polarized muons in matter (stopping time in solid ~ 10 ps, no initial loss of polarization, stop site: generally interstitial). P(0) ≅ 1

▪Magnetic moment of muon interacts with local magnetic fields (moments, currents, spins) → P(t)

▪ P(t) is characterized by precession and/or depolarization/relaxation.

▪Observe time evolution of the polarization P(t) of the muon ensemble via asymmetric muon decay: (positrons preferentially emitted along muon spin).

▪ P(t) contains information about static and dynamic properties of local environment (fields, moments,..)

$$\frac{d\vec{\mu}_\mu}{dt} = \gamma_\mu \left(\vec{\mu}_\mu \times \vec{B}(t) \right) \qquad \vec{P} = \frac{<\vec{s}>}{\frac{1}{2}\hbar}$$

$$\frac{d\vec{P}}{dt} = \gamma_\mu \left(\vec{P} \times \vec{B}(t) \right)$$

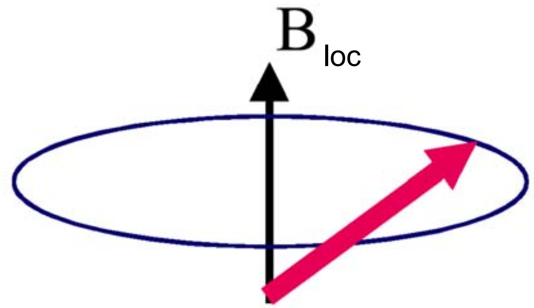

$$\omega_L = \gamma_\mu B_{loc}$$

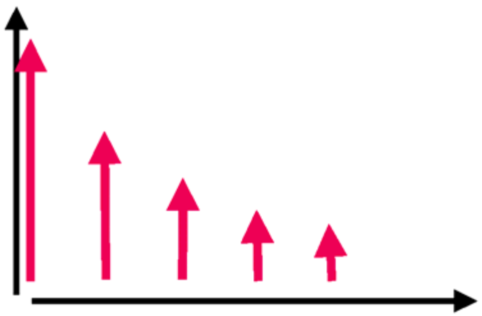

Production of polarized muons

26 ns

Parity violation in pion decay allows production of polarized muon beams.

Only "left handed" neutrinos →

in pion rest frame muon spin antiparallel to momentum.

Kinematics of pion decay at rest;
from energy and momentum conservation:

Momentum:	p_μ = 29.79 MeV/c
Kinetic energy:	E_μ = 4.12 MeV

Production of polarized muons

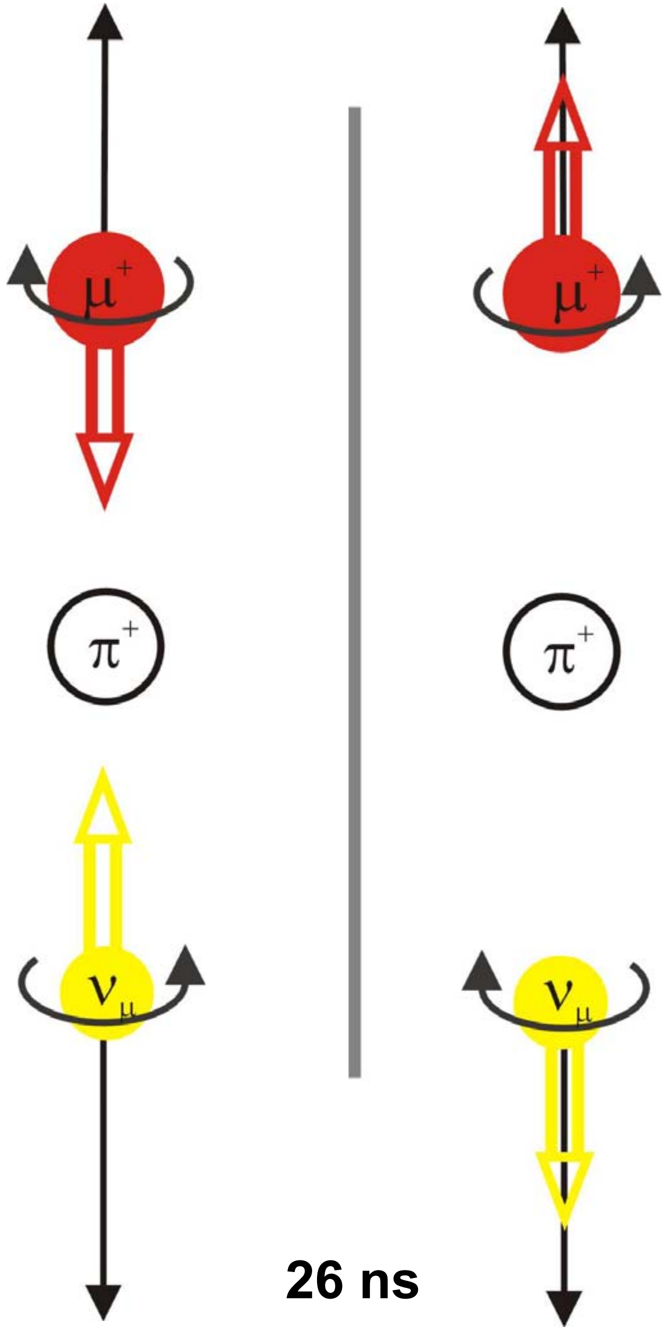

Parity violation in pion decay allows production of polarized muon beams.

Only "left handed" neutrinos →

in pion rest frame muon spin antiparallel to momentum.

Kinematics of pion decay at rest;
from energy and momentum conservation:

Momentum: p_μ = 29.79 MeV/c

Kinetic energy: E_μ = 4.12 MeV

Production of polarized muons

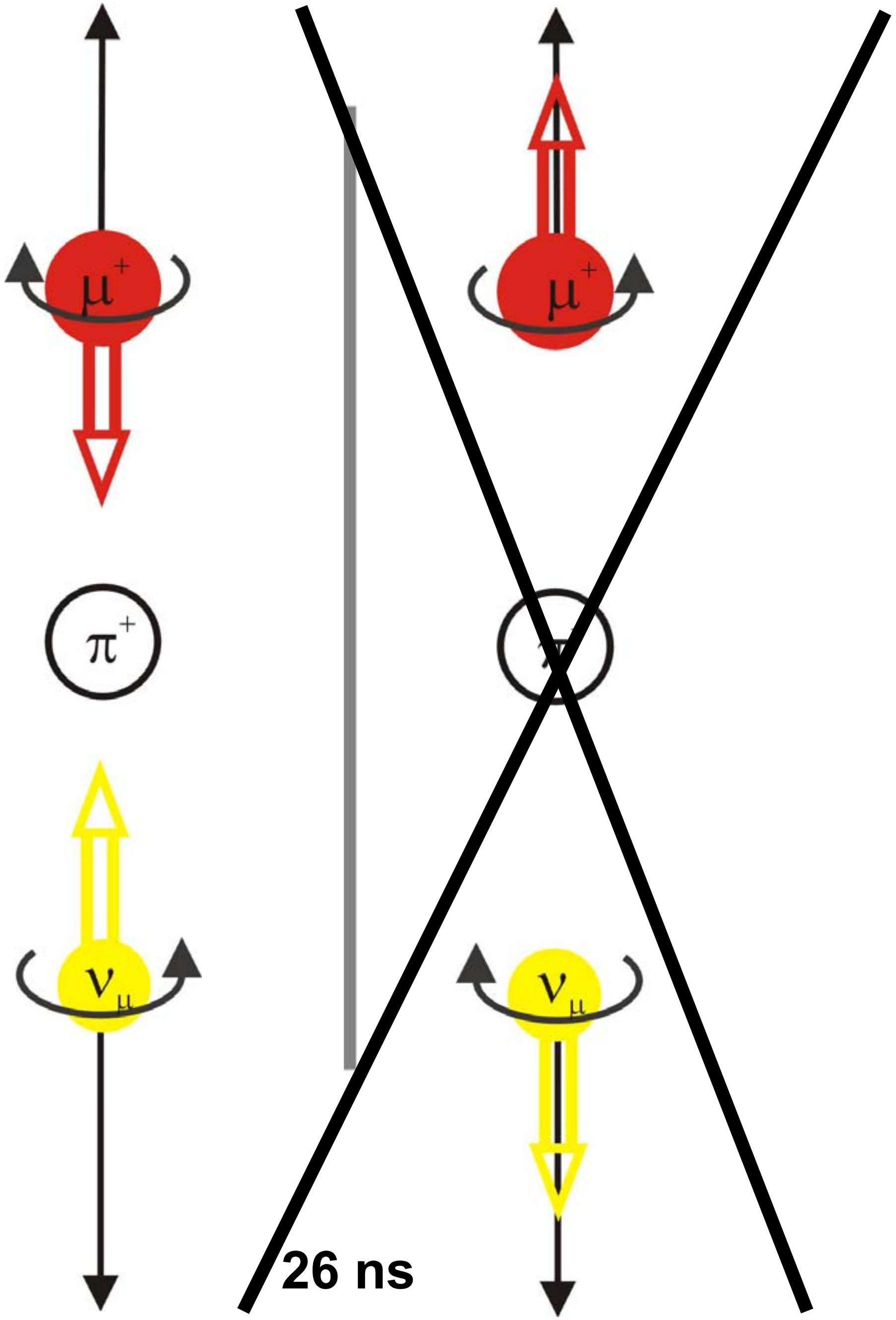

Parity violation in pion decay allows production of polarized muon beams.

Only “left handed” neutrinos →

in pion rest frame muon spin antiparallel to momentum.

Kinematics of pion decay at rest;
from energy and momentum conservation:

Momentum:	p_μ = 29.79 MeV/c
Kinetic energy:	E_μ = 4.12 MeV

Generation of polarized muons (μ^+)

2.2 mA $\cong$ 1.4 10^{16} Protons/sec

with 600 MeV

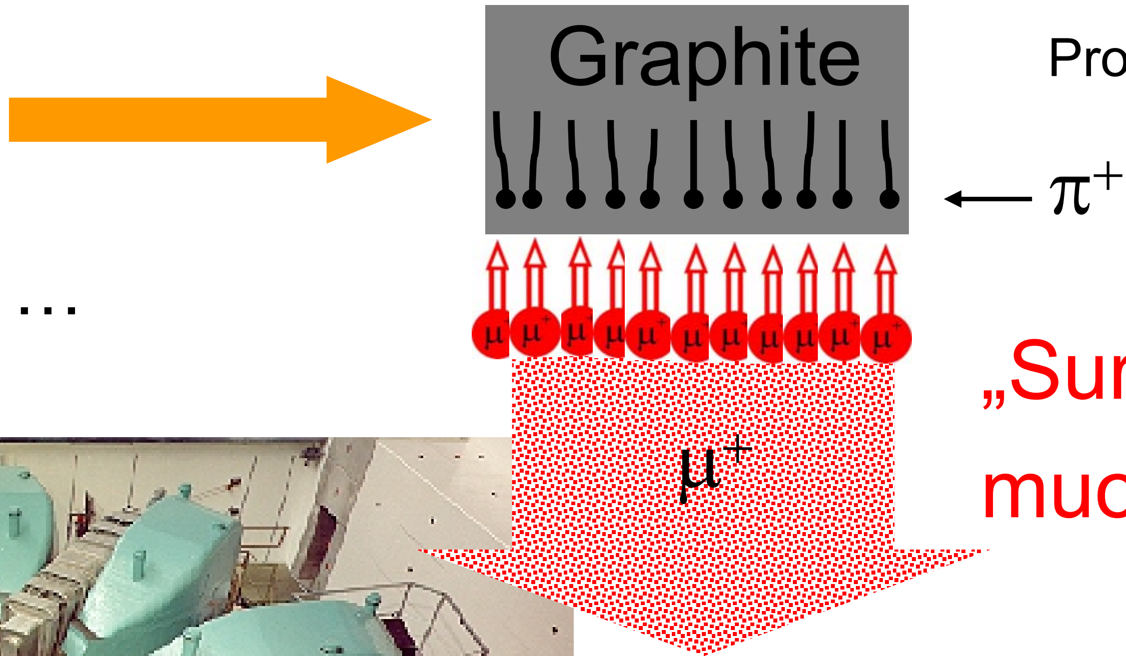

Production Target

p + C → $\pi^+ \pi^-$ p n …

„Surface“ muons

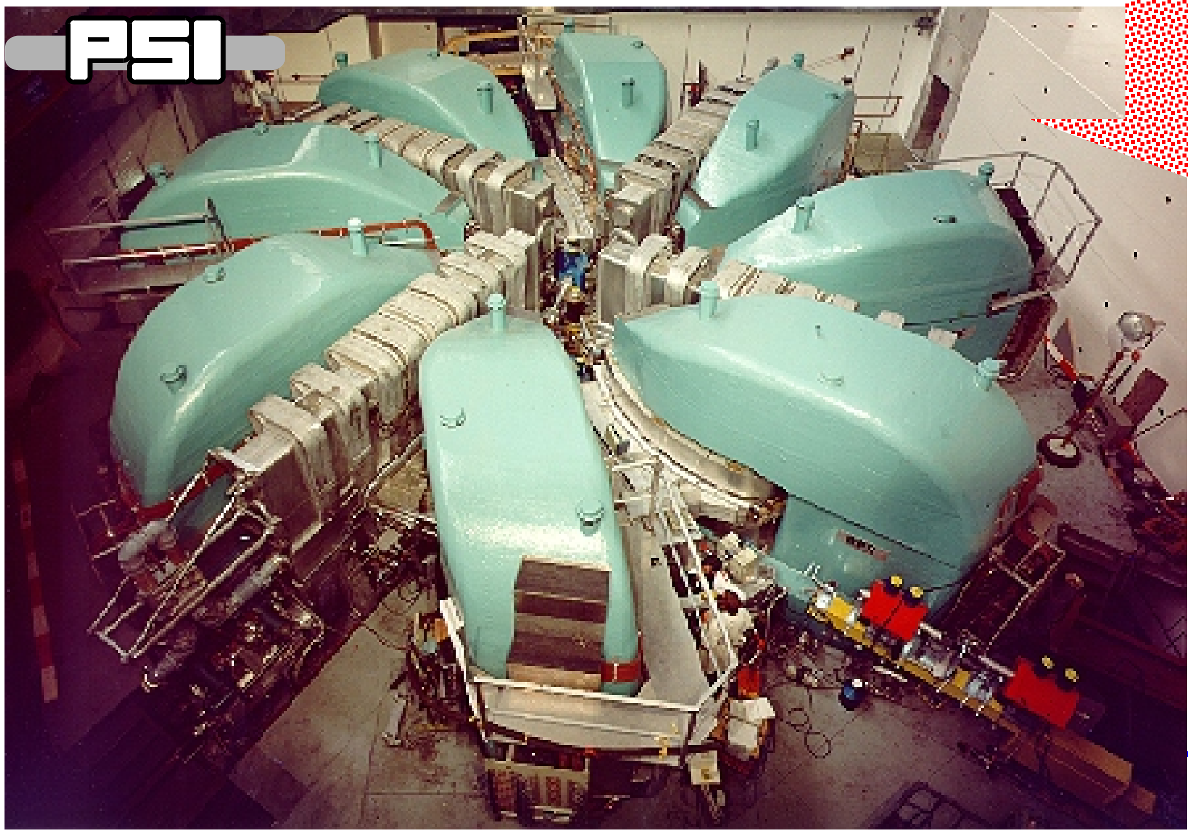

$\sim 10^7$- 10^8 μ^+/sec

100 % pol.

~ 4 MeV

generally used for “bulk” condensed matter studies

For thin film studies: eV-30 keV

SμS: The Swiss Muon Source

High Field μSR,

9.5 T, 20 mK

Until 2011 Avoided Level crossings instrument ALC

GPS

General Purpose Surface Muon Instrument

Muon energy: **4.2 MeV** (μ^+)

0.6 T, 1.8 K

Shared Beam Surface Muon Facility (Muon On REquest)

LTF

Low Temperature Facility

Muon energy: **4.2 MeV** (μ^+)

3 T, 20 mK- 4 K

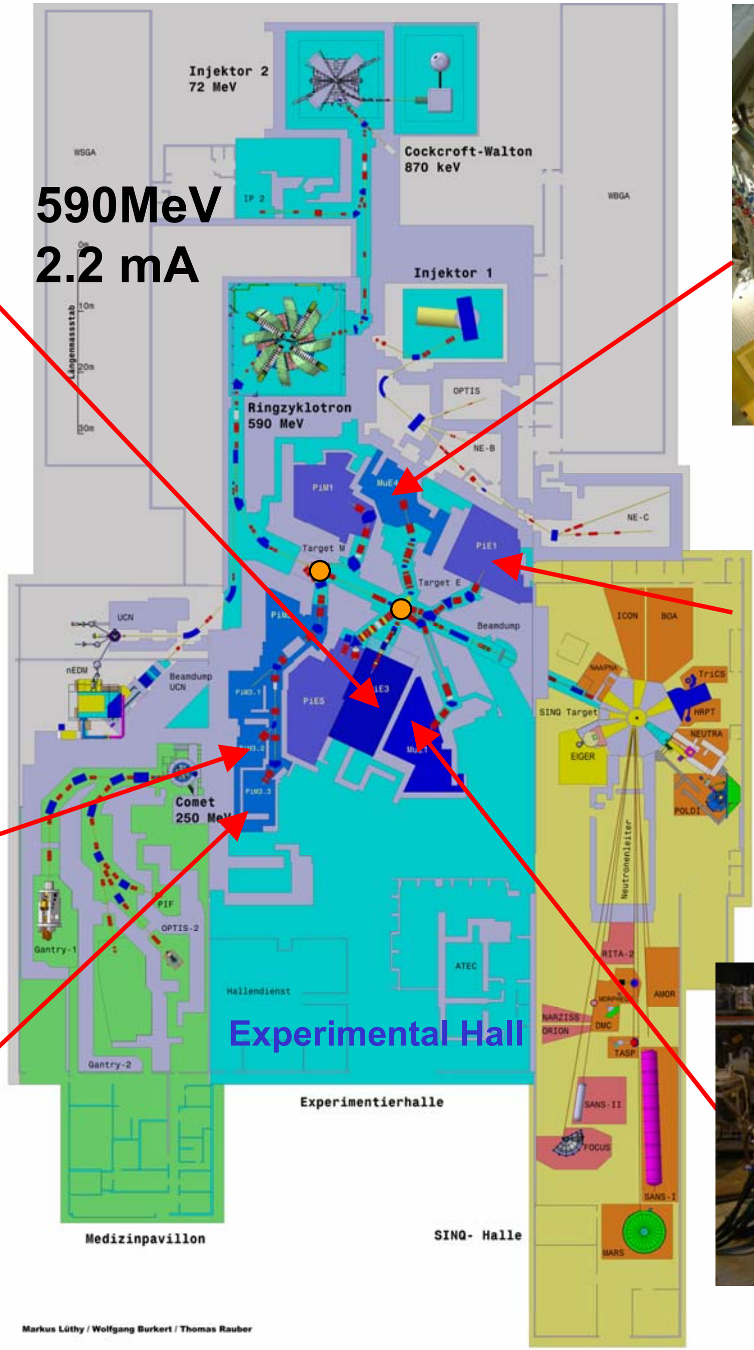

LEM

Low-energy muon beam and instrument , tunable energy (**0.5-30 keV**, μ^+), *thin-film, near-surface and multi-layer studies (1-300 nm)*

0.3 T, 2.5 K

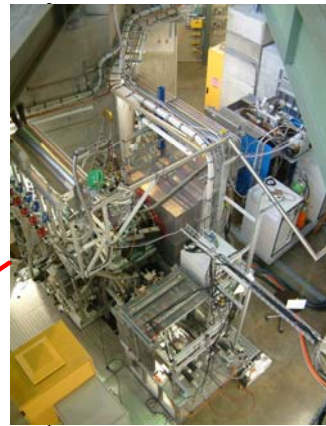

DOLLY

General Purpose Surface Muon Instrument

Muon energy: **4.2 MeV** (μ^+)

0.5 T
2 K (0.25K)

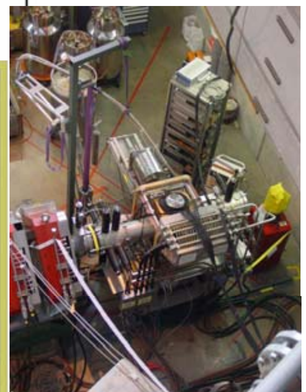

GPD

General Purpose Decay Channel Instrument

Muon energy: **5 - 60 MeV** (μ^+ or μ^-)

0.5 T,
300 mK
2.8 GPa

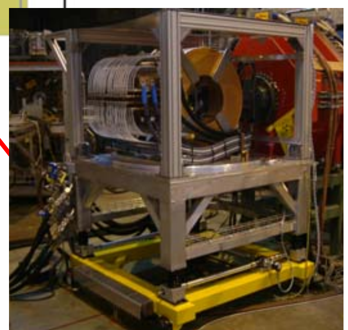

Measuring P(t): Muon Decay $\mu^+ \rightarrow e^+ + \bar{\nu}_\mu + \nu_e$

- Muon decay (life time 2.2. μs) violates parity conservation
→ asymmetric decay
- Positrons preferentially emitted along muon spin (along polarization vector of muon ensemble)

$$\frac{dN_{e^+}(\theta)}{d\Omega} \propto (1+\frac{1}{3}P\cos\theta) = (1+\frac{1}{3}\vec{P}\cdot\vec{n})$$

$\vec{n}$: direction of observation (detector position)

For $P=1$:

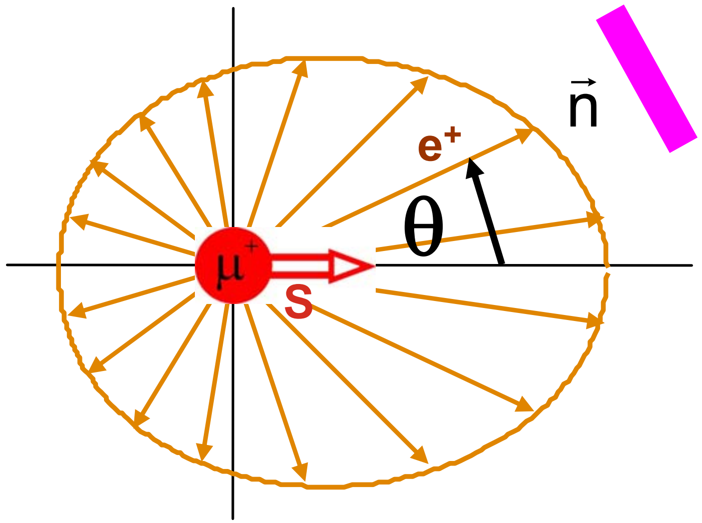

$$\frac{dN_{e^+}(\theta)}{d\Omega} \propto (1+\frac{1}{3}P\cos\theta)$$

- Measuring positrons allows to observe time evolution of the polarization P(t) of the muon ensemble
- Positron intensity as a function of time after implantation:

$$N_{e^+}(t) = N_0\left[1 + A_0 P(t)\right] e^{-\frac{t}{\tau_\mu}} \qquad P(t) = \vec{P}(t)\cdot\vec{n}$$

- A_0: Maximum observable asymmetry
  theoretically: A_0=1/3
  practically it depends on setup (average over solid angle, absorption in materials): A_0 = 0.25 - 0.30
- $A_0P(t)$ is called asymmetry: A(t)

θ : angle between spin (polarization) and positron direction

Principle of a μSR experiment

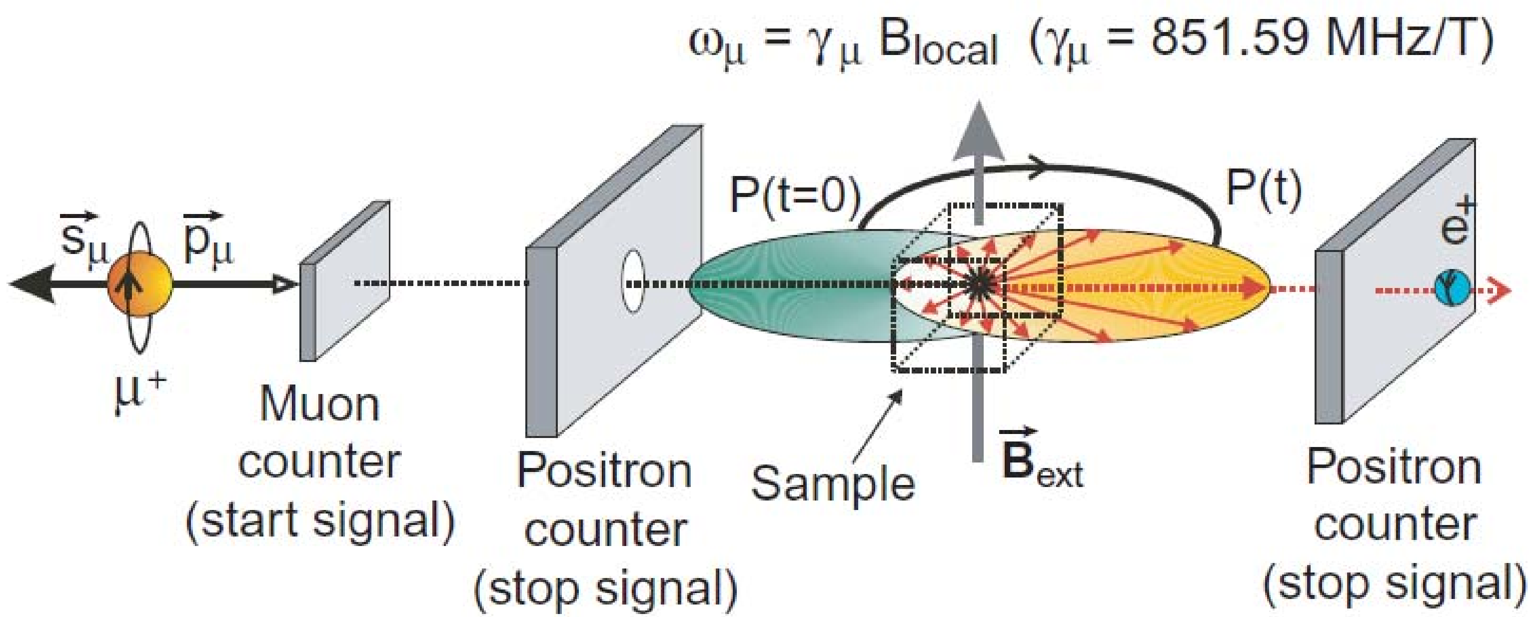

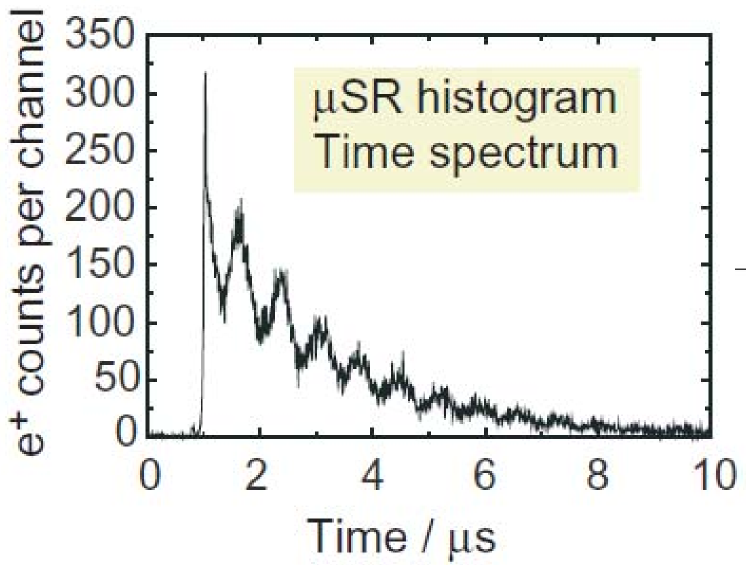

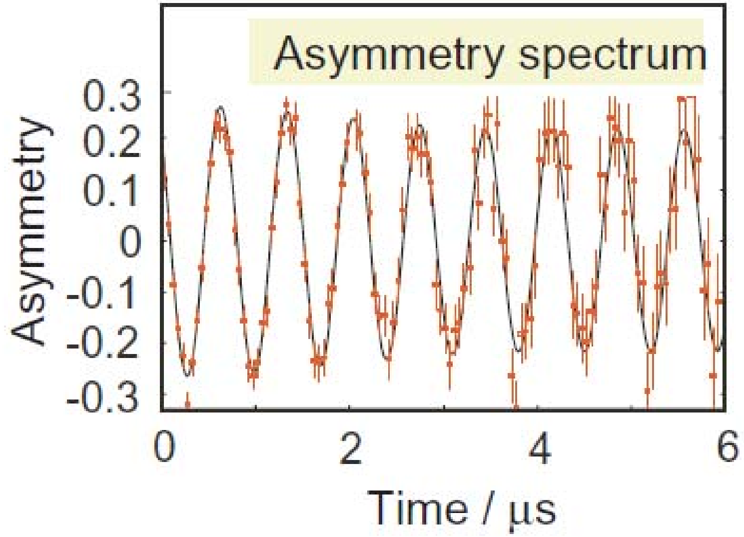

μSR: Muon Spin Rotation/Relaxation

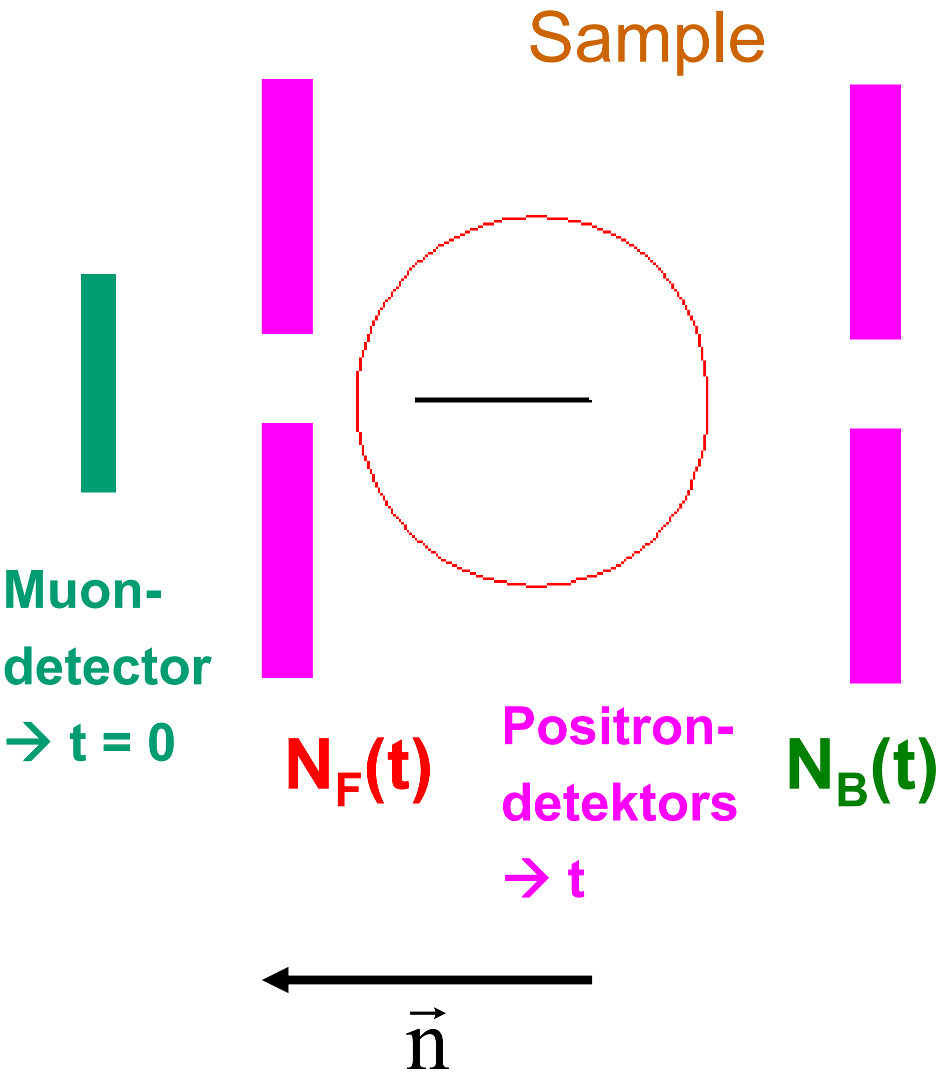

$$N_F(t) = N_0\left[1 + A_0\vec{P}(t)\cdot\vec{n}\right]\, e^{-\frac{t}{\tau_\mu}}$$

$$N_B(t) = N_0\left[1 - A_0\vec{P}(t)\cdot\vec{n}\right]\, e^{-\frac{t}{\tau_\mu}}$$

$$\frac{N_F(t) - N_B(t)}{N_F(t) + N_B(t)} = AP(t) \qquad (P(t) = \vec{P}(t)\cdot\vec{n})$$

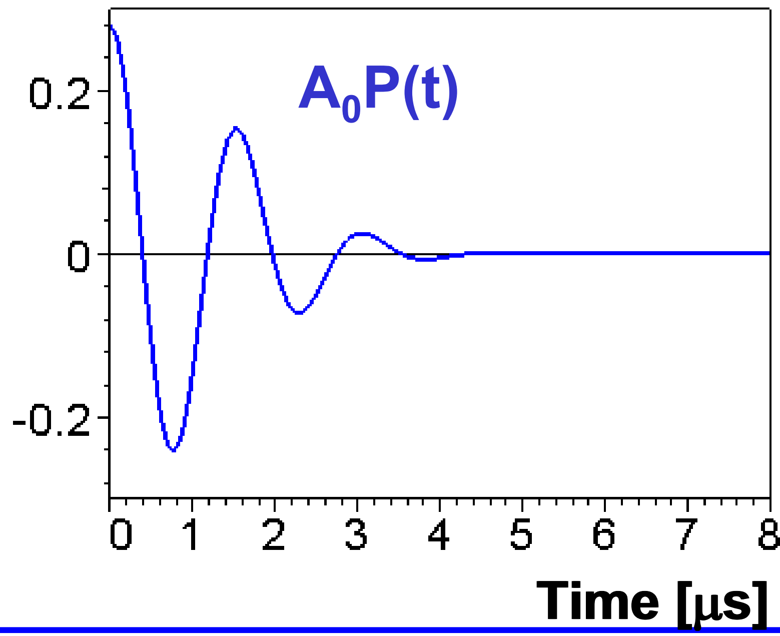

TF: Transverse Field geometry

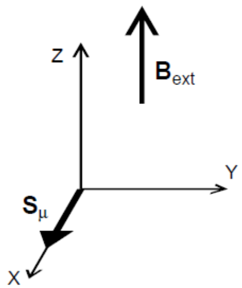

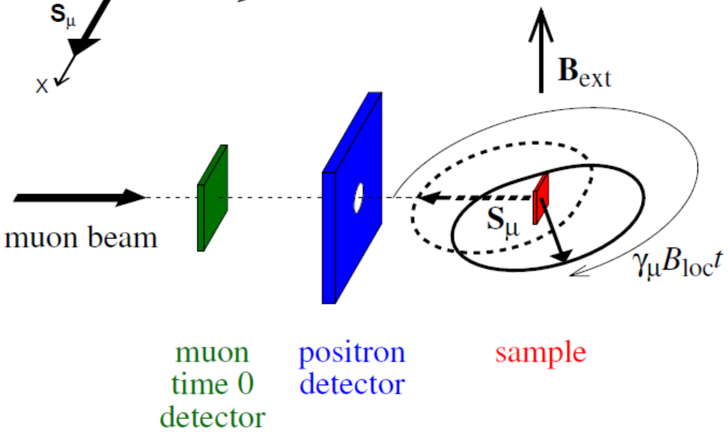

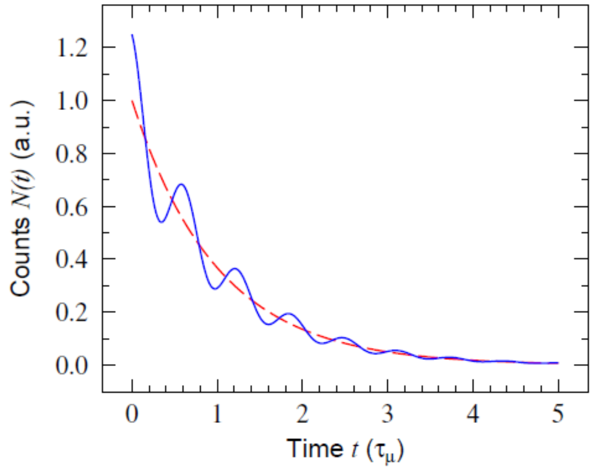

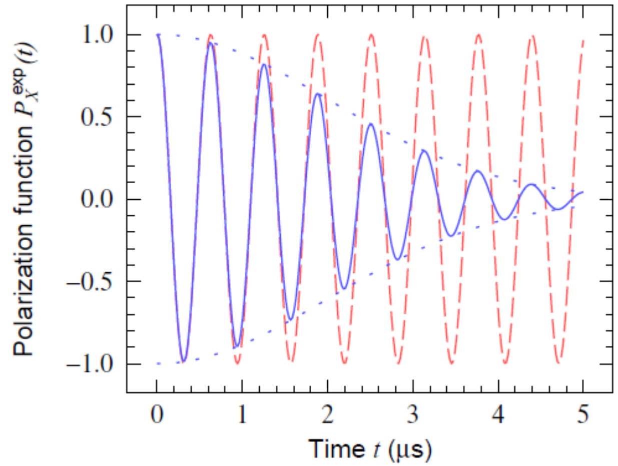

ZF and LF: Zero field and Longitudinal Field geometry

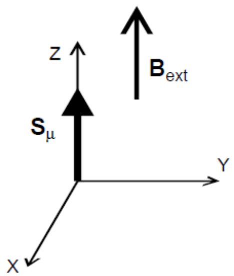

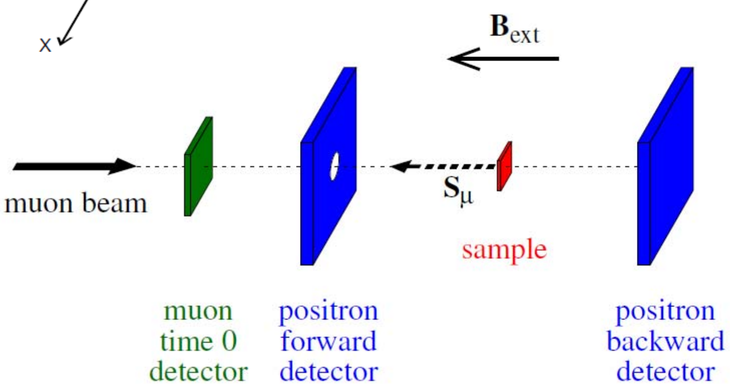

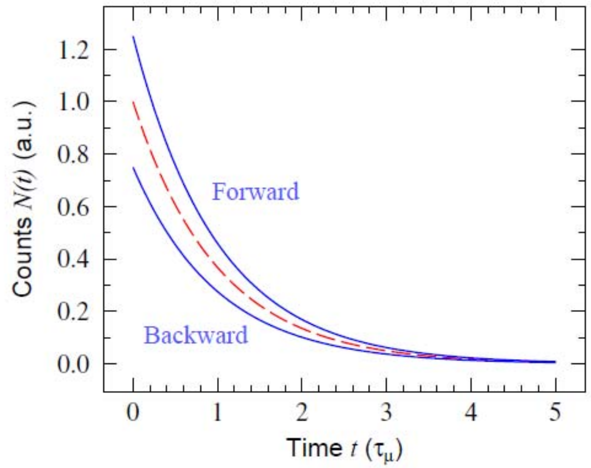

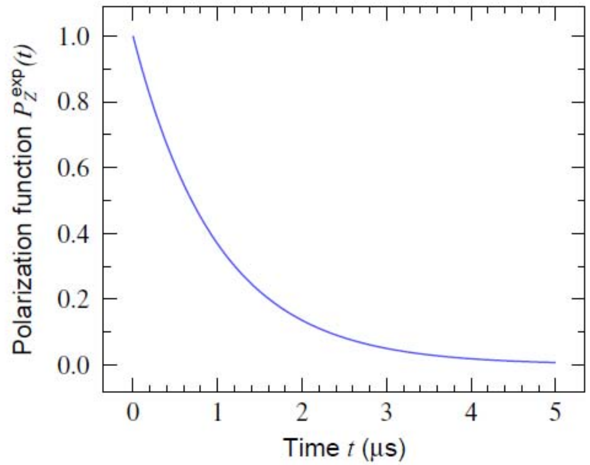

P(t): time evolution of polarization

$$\frac{d\vec{P}}{dt} = \gamma_\mu \left(\vec{P} \times \vec{B}(t)\right)$$ $\vec{B}$ is the total field at muon site (i.e. including applied field)

Simplest case:

All muons in the sample experience the same static field $\vec{B}=(B_x, B_y, B_z)$

Static means: $\vec{B}$ does not change over obervation time (5-10 τ_μ): $\frac{B(t)}{\frac{dB(t)}{dt}} >> \tau_\mu$

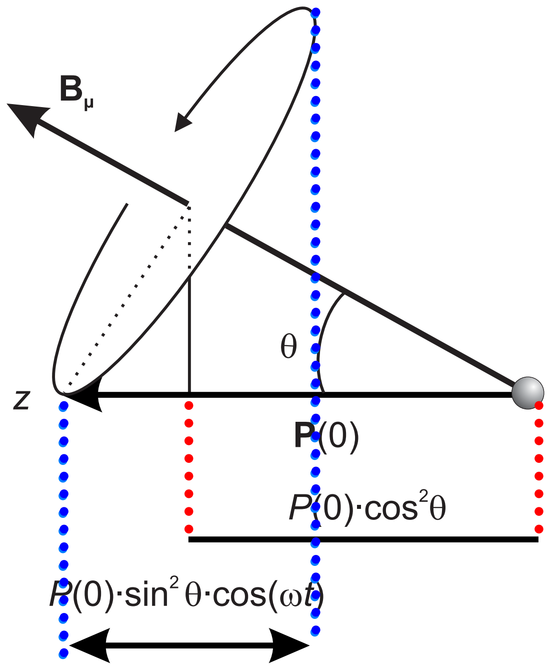

$\vec{P}(0) \parallel \hat{z} \equiv \hat{n}$ (Direction of observation)

$$P_{\vec{B}}(t) = \cos^2\theta + \sin^2\theta\cos(\omega_L t) = \frac{B_z^{\,2}}{B^2} + \frac{B_x^{\,2} + B_y^{\,2}}{B^2}\cos(\gamma_\mu B t)$$

$\omega_L \equiv \gamma_\mu B$ Larmor Frequency (Spin precession frequency)

P(t): time evolution of polarization

$$\frac{d\vec{P}}{dt} = \gamma_\mu \left(\vec{P} \times \vec{B}(t)\right)$$

$\vec{B}$ is the total field at muon site (i.e. including applied field)

In case the muons experience a field distribution $p(\vec{B})$

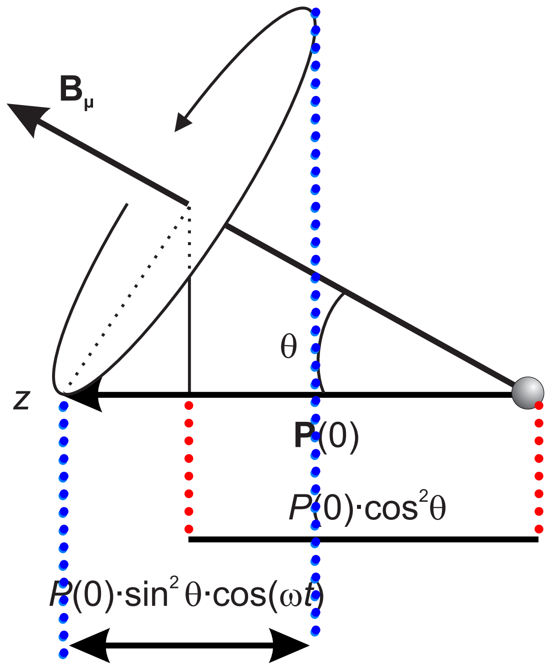

$$P(t) = \int p(\vec{B}) P_{\vec{B}}(t) d^3B = \int p(\vec{B}) \left[\frac{B_z^{\,2}}{B^2} + \frac{B_x^{\,2} + B_y^{\,2}}{B^2} \cos(\gamma_\mu B t) \right] d^3B$$

Magnetism: polycristalline sample

$|\vec{B}|$ equal all over the sample, isotropic direction:

$$P(t) = \frac{1}{4\pi}\int \cos^2\theta + \sin^2\theta\cos(\gamma_\mu|\vec{B}|t)d\varphi\, d(\cos\theta) = \frac{1}{3} + \frac{2}{3}\cos(\gamma_\mu|\vec{B}|t)$$

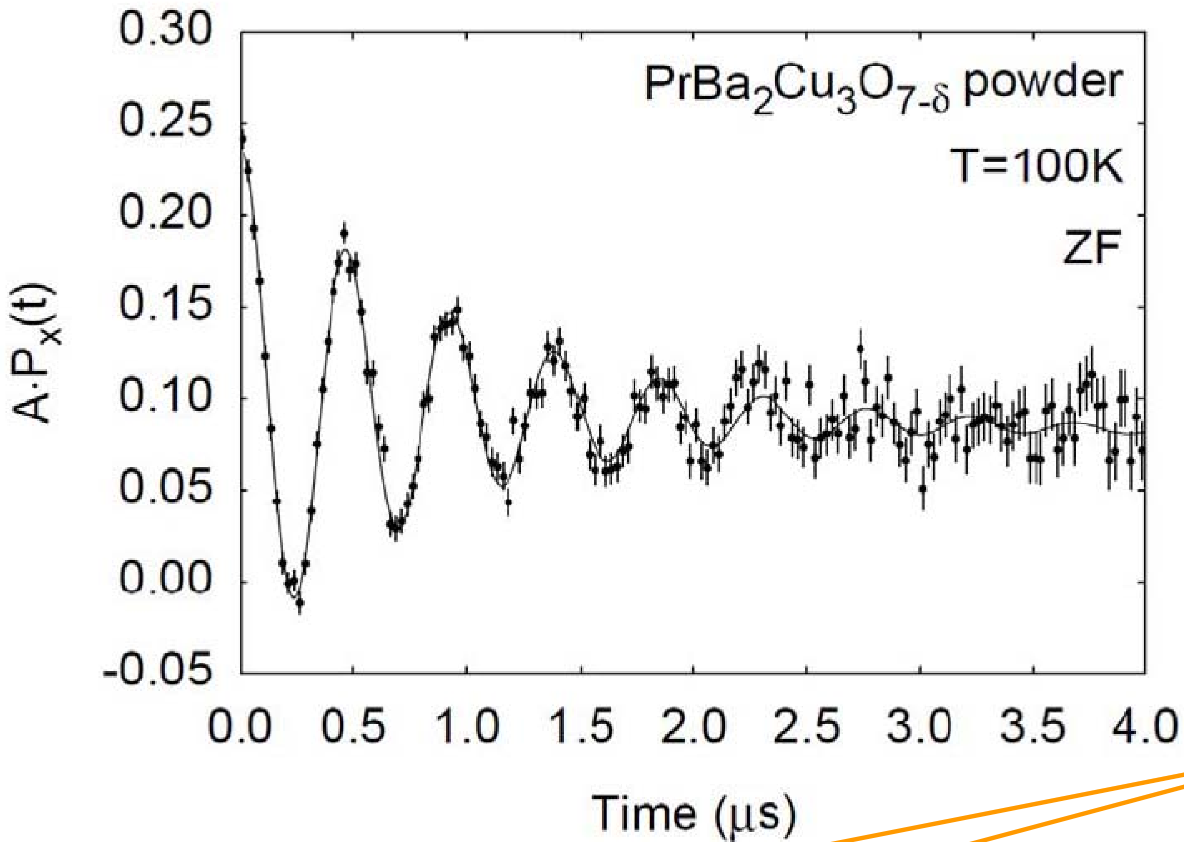

Damping, Depolarization

$$A_0P(t) = A_0\left[e^{-\lambda_L t}\frac{1}{3} + e^{-\lambda_T t}\frac{2}{3}\cos(\gamma_\mu|\vec{B}|t)\right]$$

Microscopic magnetometry

$B_{ext}=0$

$(C_{13}H_{23}O_2NO)_2$

Organic antiferromagnet

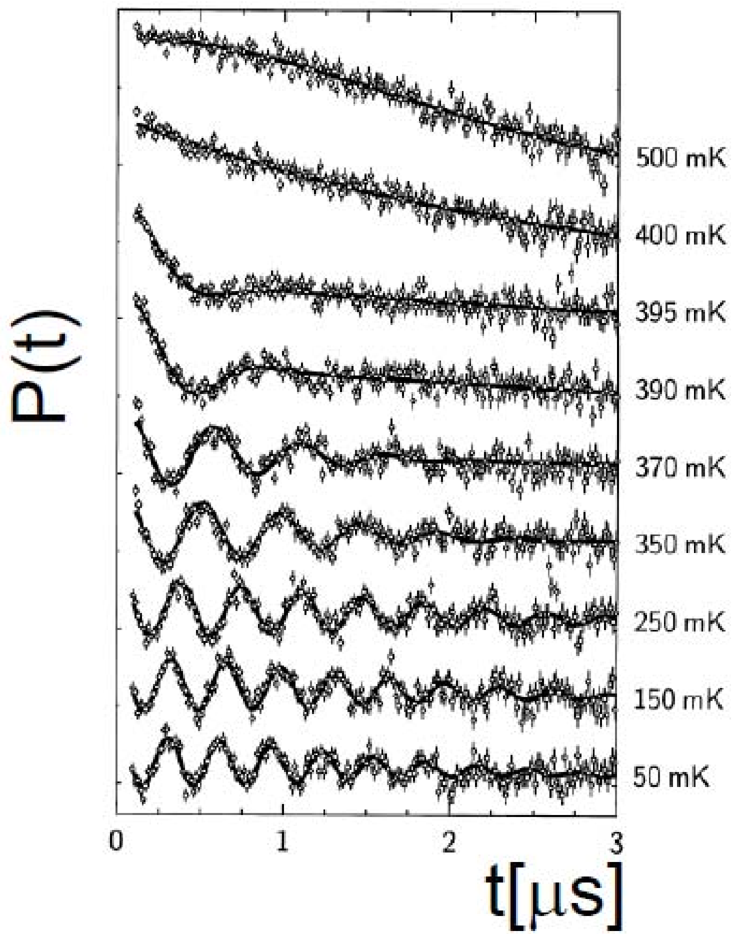

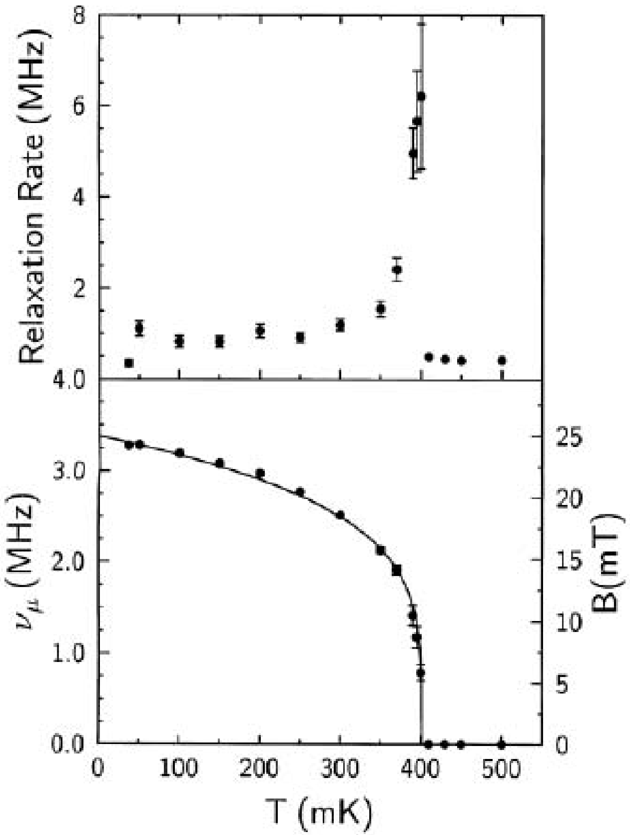

$$P(t) = a_L(t) + a_T e^{-\lambda t}\cos(2\pi\nu_\mu t)$$

$$\lambda = \frac{1}{T}$$ relaxation rate, $[\mu s^{-1}]$ or [MHz]

S. Blundell et al., Physica B (2000)

Local field in magnetic materials

Internal field: generally sum of dipolar:

$$\vec{B}_{dip}(\vec{r}) = \frac{\mu_0}{4\pi} \frac{3(\vec{\mu}_i \cdot \vec{r}_{1\mu}) \cdot \vec{r}_{1\mu} - \vec{\mu}_i r_{1\mu}^2}{r_{1\mu}^5}$$

$$B_{dip} \approx \frac{\mu_0}{4\pi} \frac{\mu_i}{r_{1\mu}^3} \approx \frac{\mu_i[\mu_B]}{d^3[A^3]} \ T \approx 0.1T$$

and contact field (spin density at muon site):

$$\vec{B}_{hf}(\vec{r}_\mu) = \frac{2\mu_0}{3} \mu_B \rho_{spin}(\vec{r}_\mu) \cong \frac{2\mu_0}{3} \mu_B \left|\varphi(\vec{r}_\mu)\right|^2 < \vec{s} >$$

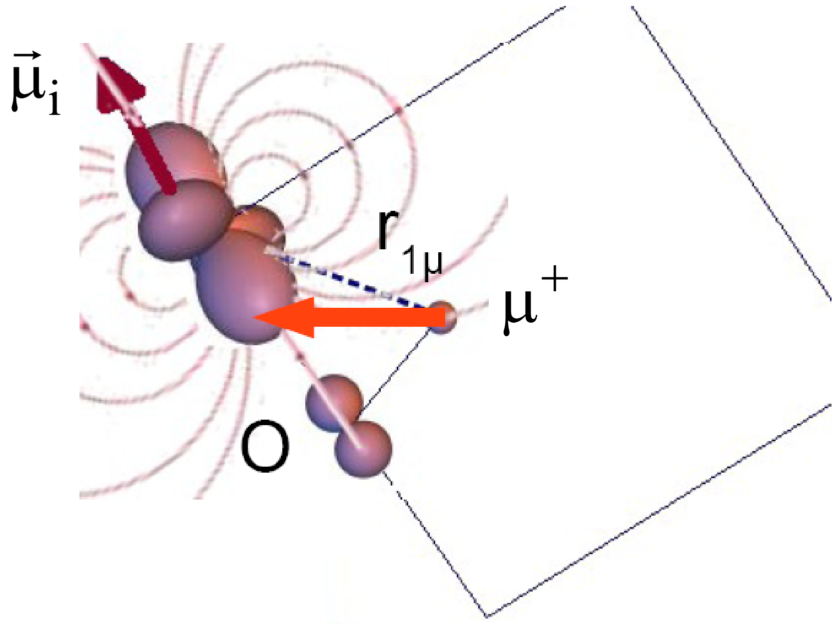

High sensitivity:

μSR time window 10-20 μs

$\rightarrow \nu_\mu \cong 50$ kHz detectable

$$\rightarrow B = \frac{2\pi}{\gamma_\mu} \nu_\mu \approx 0.1 \text{mT (Gauss)}$$

(corresponds to $0.001\mu_B$ or nuclear moments μ_n)

Inhomogeneous materials: determination of volume fraction

Homogeneous:

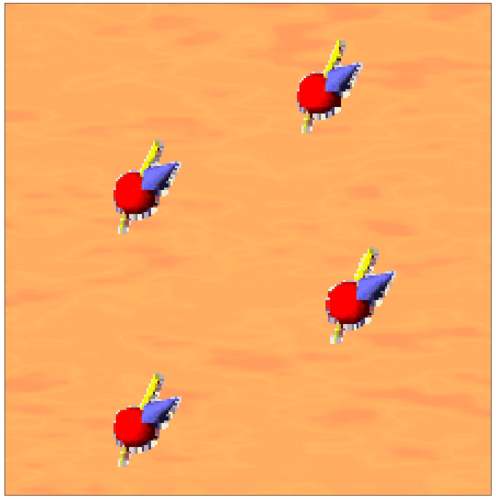

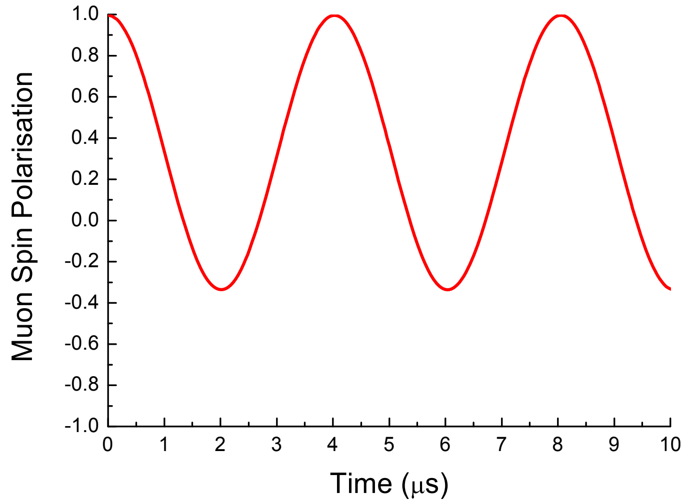

Inhomogeneous:

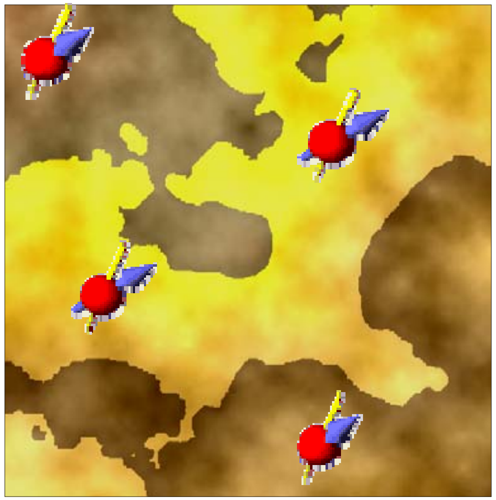

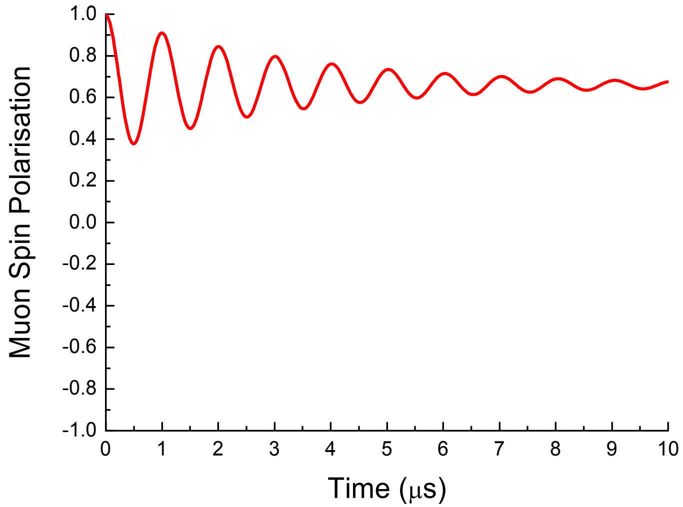

Amplitude a = Magnetic volume fraction

Frequency ω = Local field, size of magnetic moments

Damping λ, σ = inhomogeneity of magnetic regions

Example URu_2Si_2

Neutron scattering:

F. Bourdarot et al., condmat/0312206

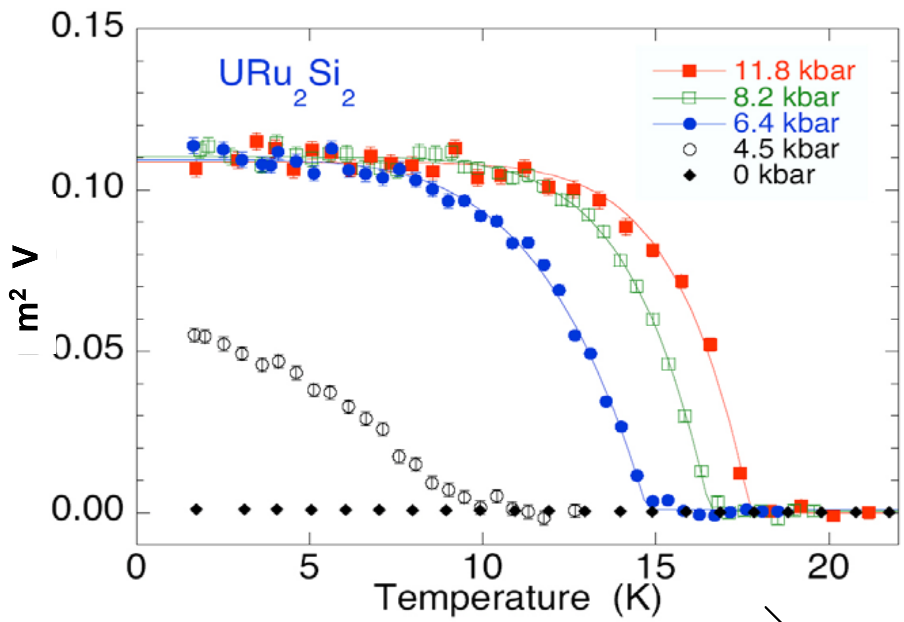

Muon Spin Rotation:

A. Amato et al., J. Phys.: Condens. Matter **16** (2004) S4403

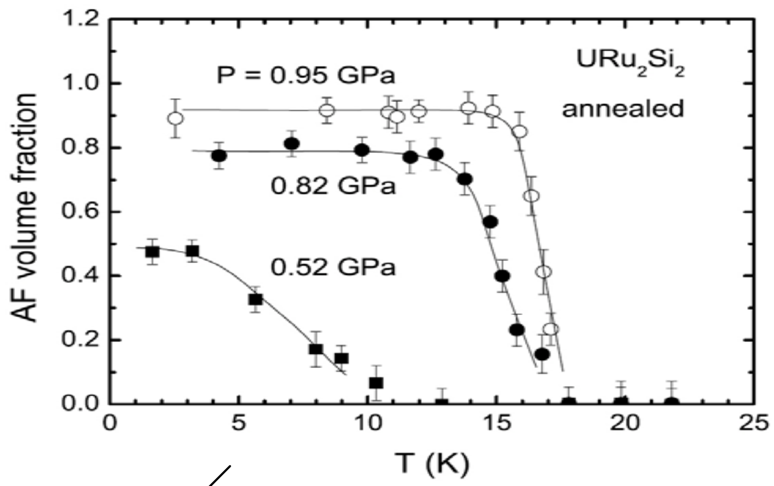

Phase separation in magnetic and non magnetic volumes

Only the combination of neutron and muon data allows the correct interpretation of the data

Example: $RuSr_2GdCu_2O_8$

Resistivity:
(**Superconductivity**)

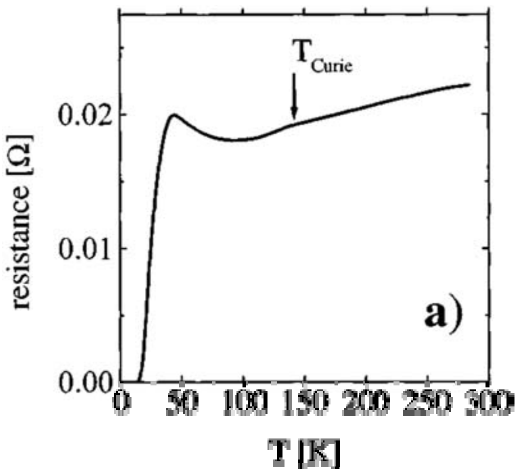

Magnetization:
(**Ferromagnetism**)

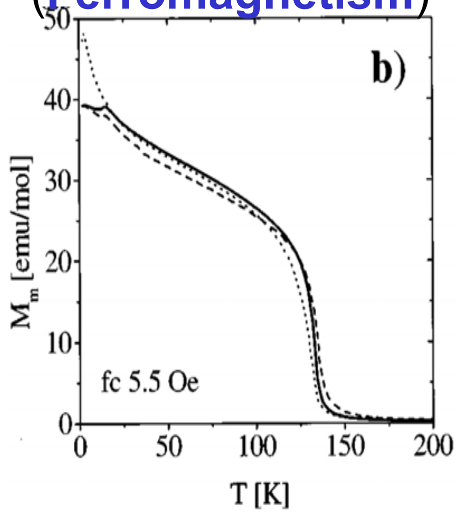

μSR:

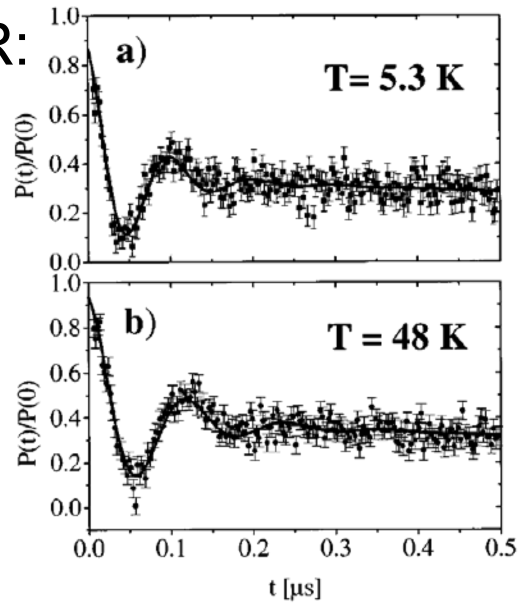

~100%
magnetic volume

Microscopic coexistence of superconductivity and magnetism

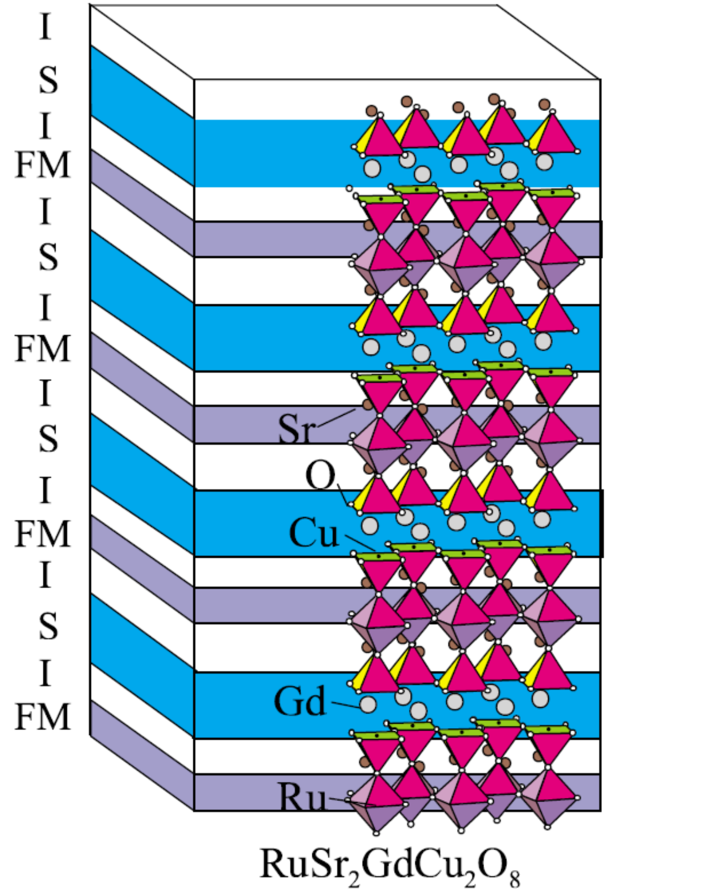

Structure:
T. Nachtrab et al., Phys. Rev. Lett. **92** (2004) 117001

C. Bernhard et al., Phys. Rev. B 59 (1999) 14099

Vortex state of a type II superconductor

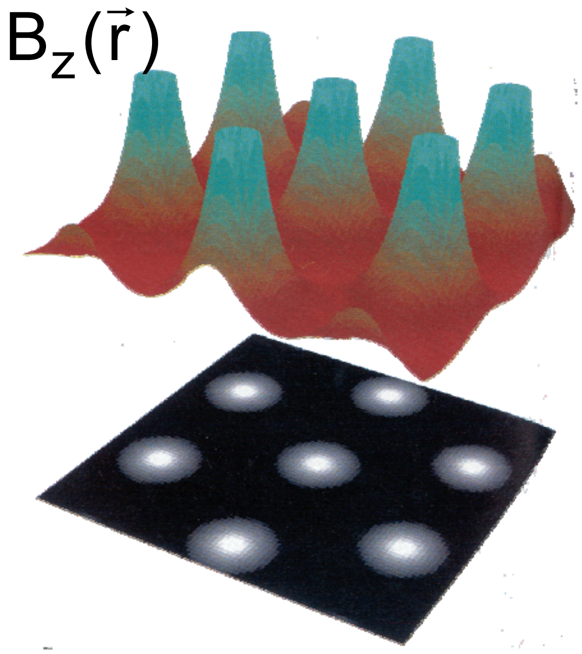

1 vortex:

$$\Phi_o = \frac{h}{2e}$$

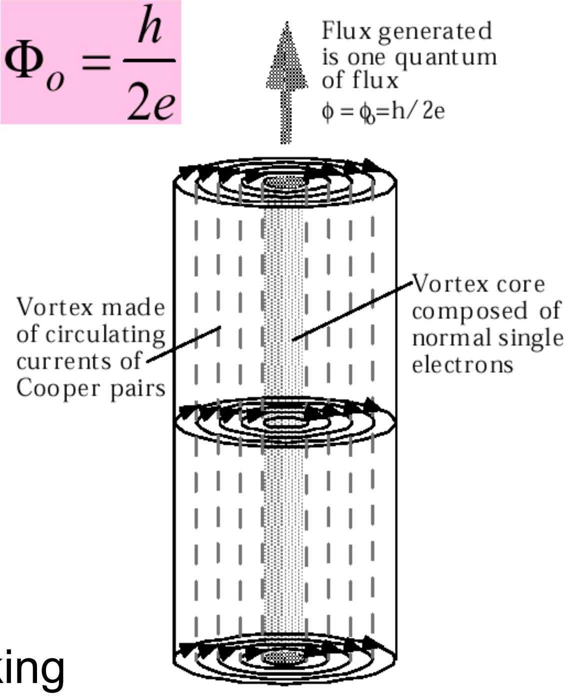

Vortex of supercurrents

$$\kappa \equiv \frac{\lambda}{\xi} > \frac{1}{\sqrt{2}}$$

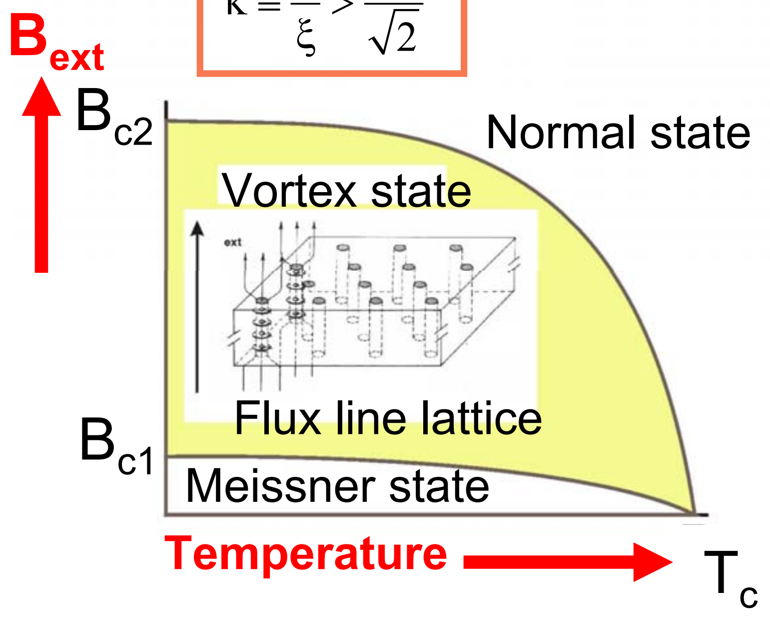

B(r) can be obtained from a modified London equation taking into account the flux generated by the regular array of vortices

$$\Delta\vec{B}(\vec{r}) - \frac{\vec{B}(\vec{r})}{\lambda^2} = \frac{\Phi_0}{\lambda^2}\sum_{\vec{R}}\delta(\vec{r}-\vec{R})\hat{z}$$

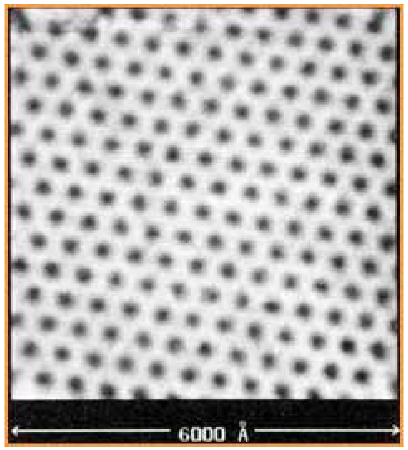

Surface image by Scanning Tunnel Microscopy
$NbSe_2$, 1T, 1.8K
H. F. Hess et al. Phys. Rev. Lett. 62, 214 (1989)

μSR in the vortex state

Normal state

Vortex-state

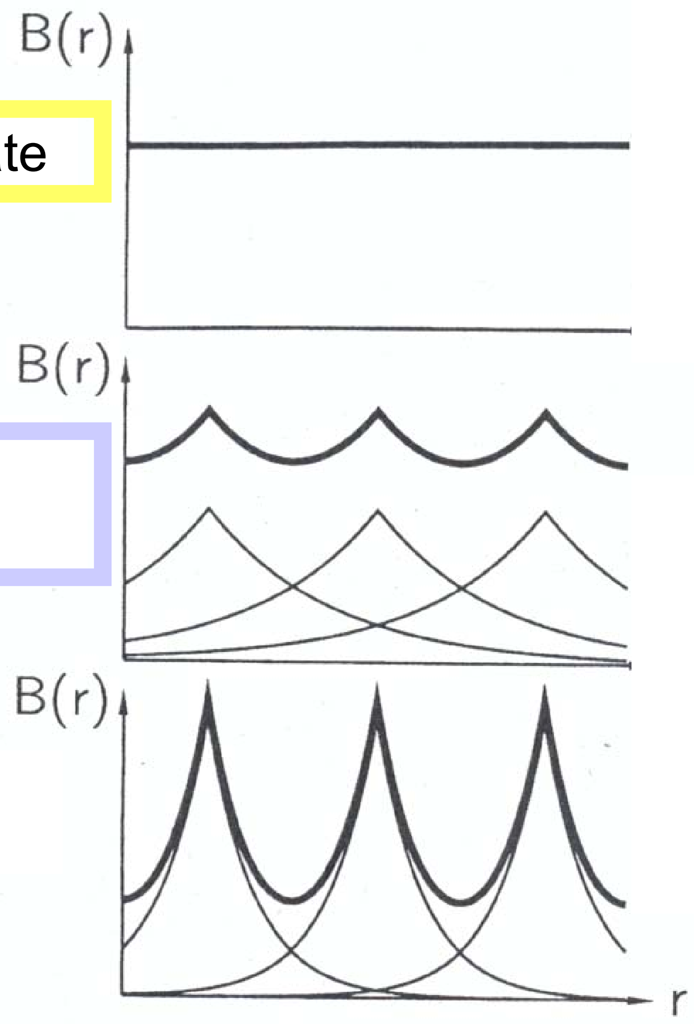

$YBa_2Cu_3O_{6.95}$

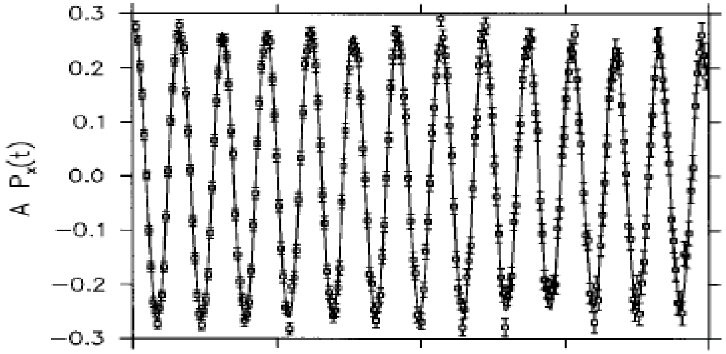

$$AP_x(t) = A\cos(\gamma_\mu Bt + \Phi)$$

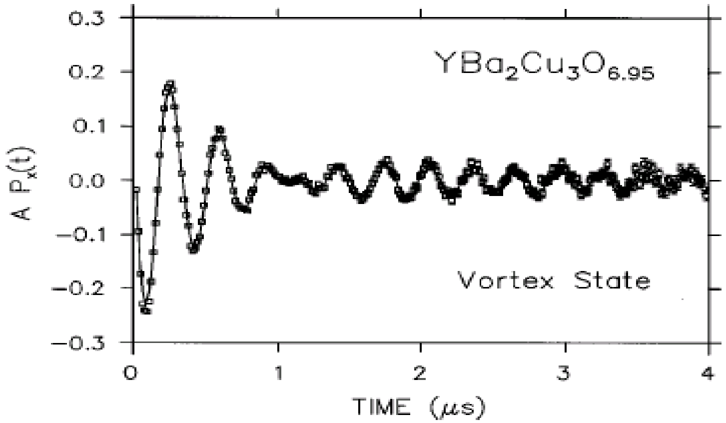

$$P_x(t) = \frac{1}{N}\sum_{i=1}^{N}\cos(\gamma_\mu B(\vec{r}_i)t + \phi)$$

$$P_x(t) = \int p(B_z)\cos(\gamma_\mu B_z t + \phi)\, dB_z$$

Field distribution vortex state

$$P_x(t) = \int p(B_z)\cos(\gamma_\mu B_z t + \phi)\, dB_z$$

$p(B_z)$: field distribution

(field averaged over all muon sites)

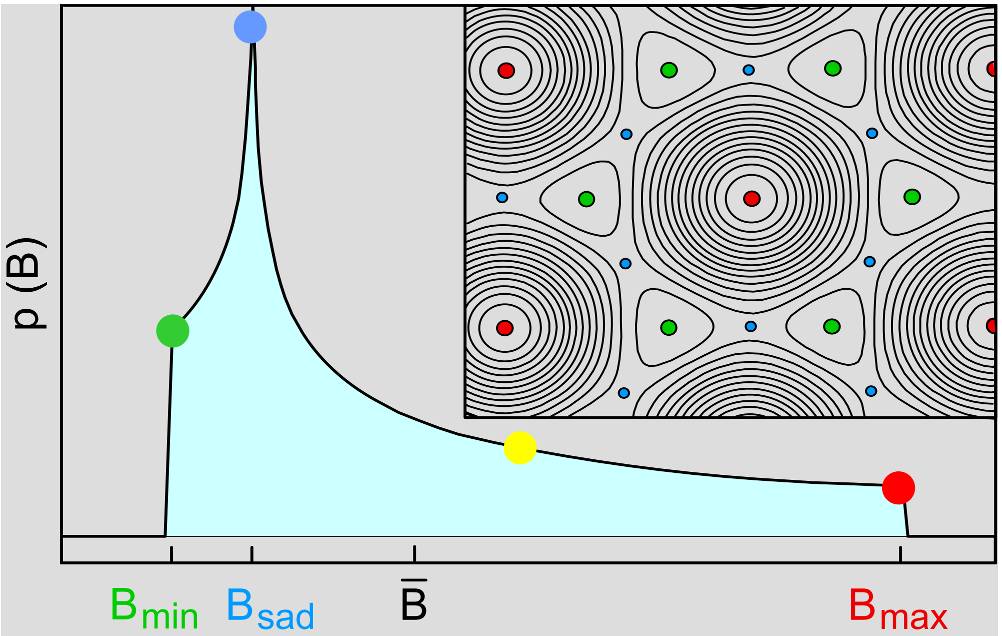

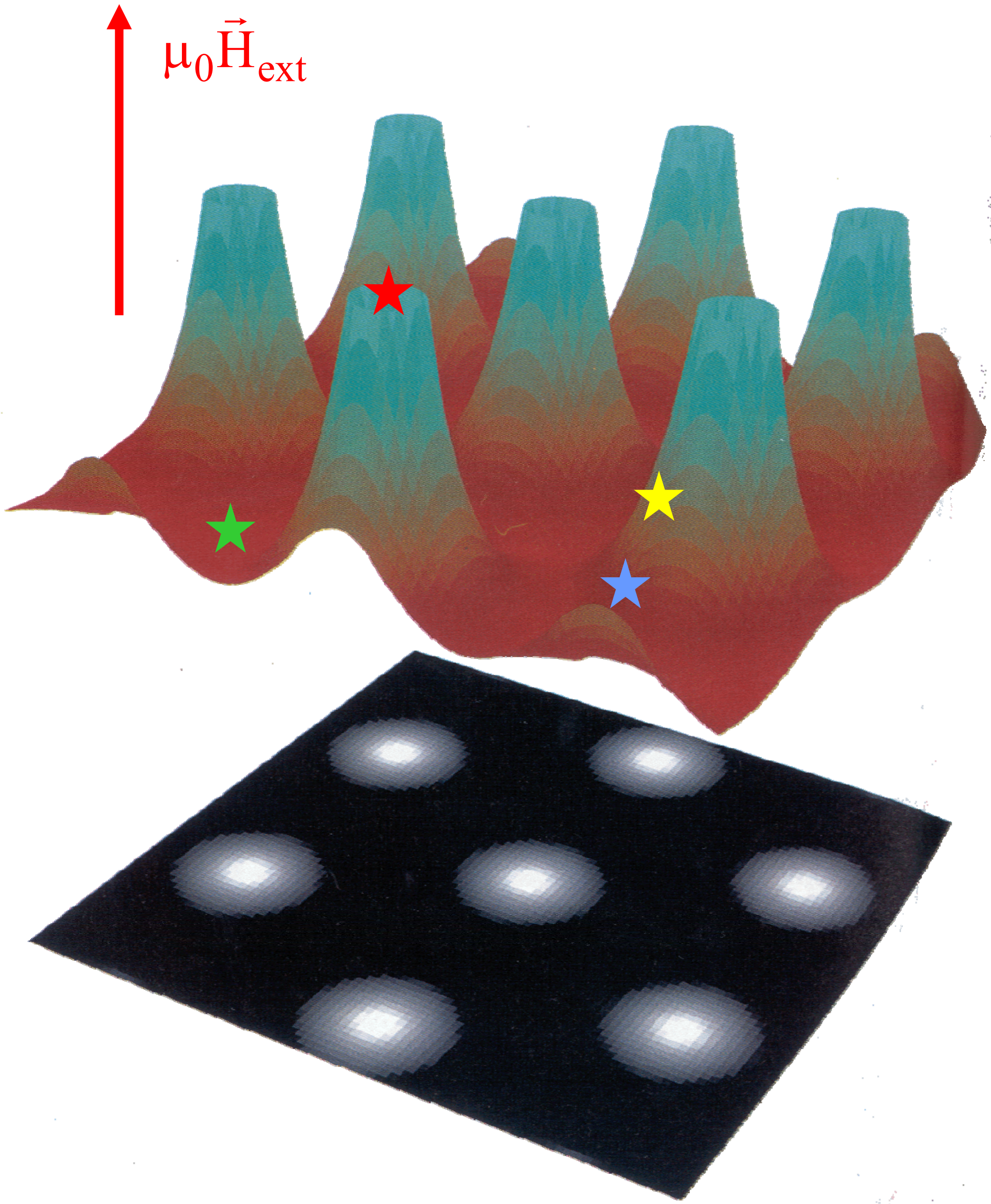

*Bishop et al., Scientific American **48** (1993)*

Field distribution in vortex state

$$P_x(t) = \int p(B_z)\cos(\gamma_\mu B_z t + \phi)\, dB_z$$

$p(B_z)$: microscopic magnetic field distribution $p(B_z) \longleftrightarrow B_z(r)$

= Fourier tranform of time evolution of polarization P(t)

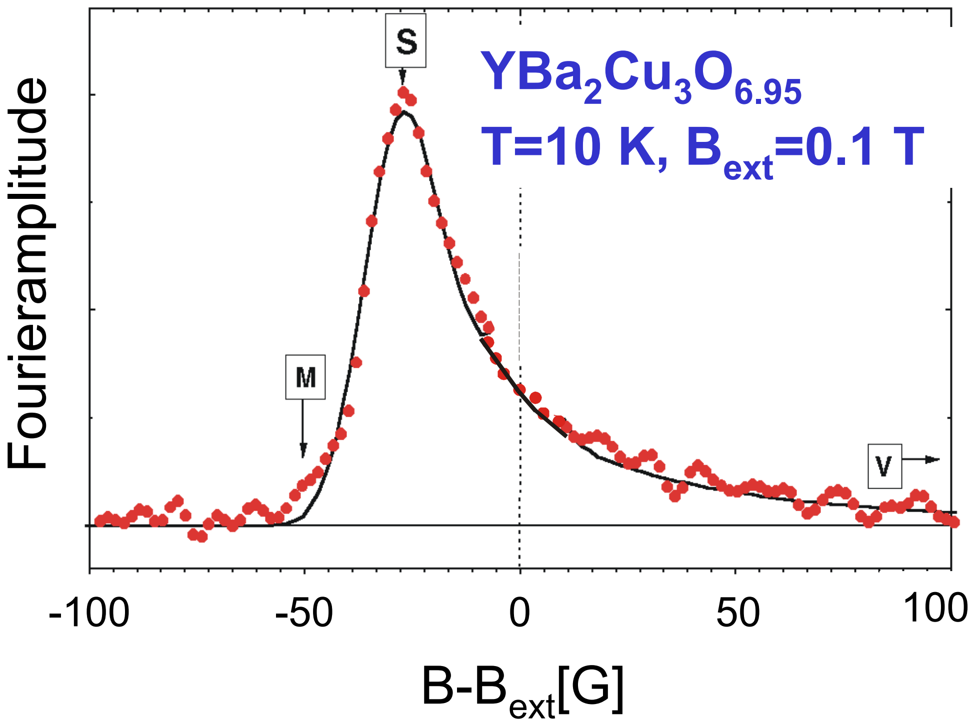

- Structure, symmetry of the Flux line lattice
- Vortex motion
- Charakteristic lengths: magnetic penetration depth λ, radius of the vortex core (coherence length)
- Classification scheme of superconductors

Spatial dependence of field and field width

$$\Delta\vec{B}(\vec{r}) - \frac{\vec{B}(\vec{r})}{\lambda^2} = \frac{\Phi_0}{\lambda^2}\sum_{\vec{R}}\delta(\vec{r}-\vec{R})\hat{z}$$

can be explicitely solved in reciprocal space:

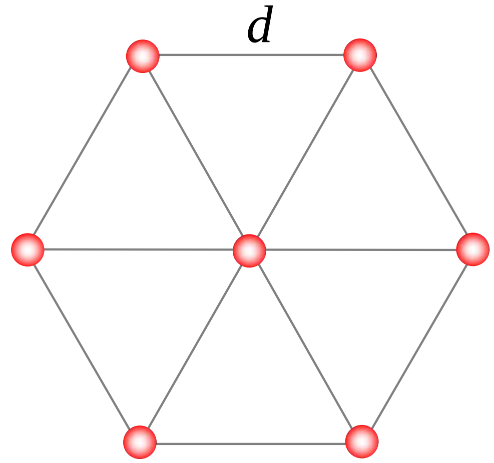

$$B_z(\vec{r}) = \sum_{\vec{k}} \frac{<B>}{1+\lambda^2 k^2} e^{i\vec{k}\vec{r}}$$

and the second moment calculated

$$<\Delta B_z^2> \;=\; <B_z^2> - <B_z>^2$$

we obtain:

$$<\Delta B_z^2> \;=\; 0.00371\frac{\Phi_0^2}{\lambda^4}$$

A μSR measurement of the second moment of the field distribution allows to determine the London penetration depth λ.

$$\rightarrow \lambda(T) = \sqrt{\frac{m^*}{\mu_0 e^2 n_s(T)}}$$

n_s: supercarrier density, m*: effective mass

Field distribution in vortex state

Single crystals:

asymmetric field distribution.

Allow to study anisotropic properties of high temperature superconductors

Sonier et al., PRL 83, 4156 (1999)

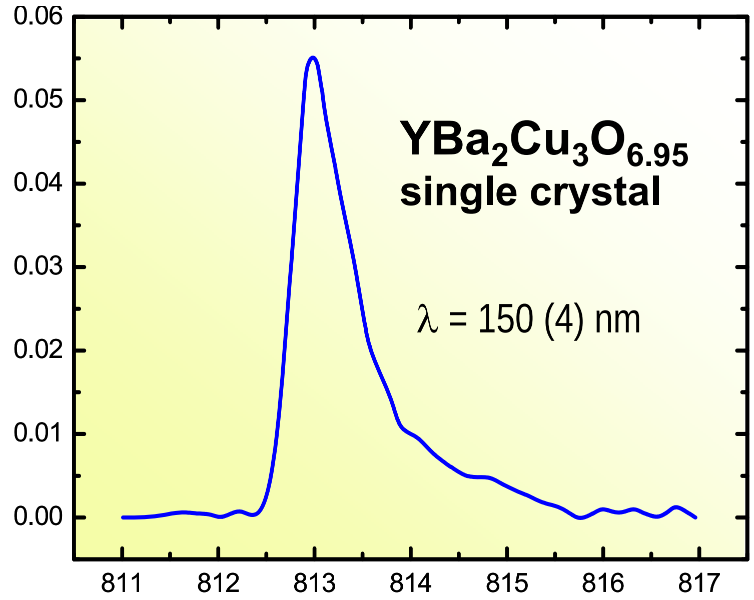

Polycrystals or sintered samples: large density and disorder of pinning sites → strong smearing of the field distribution. Can be approximated by Gauss distribution

Pümpin et al., Phys. Rev. B 42, 8019 (1990)

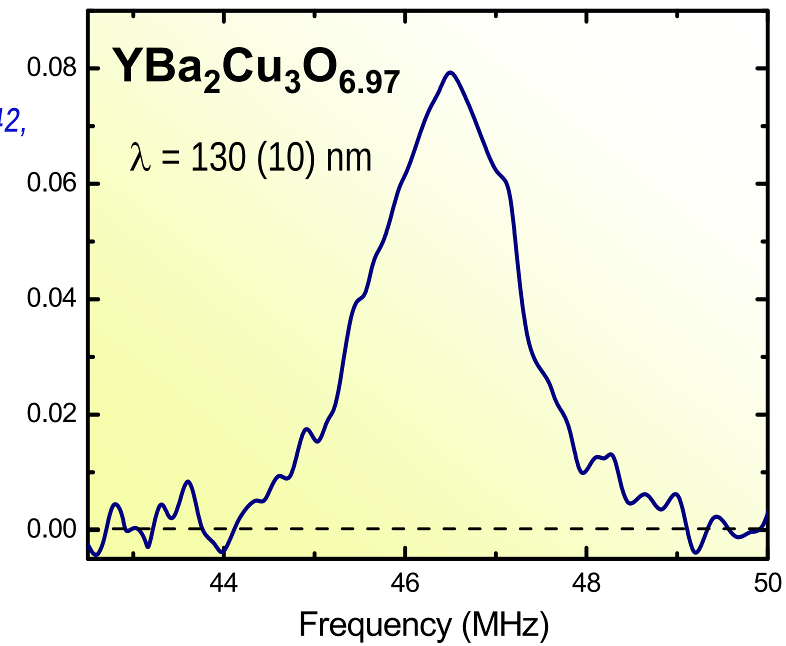

Gauss field distribution and polarization

Gaussian damped precession

$$P(t) = e^{-\frac{\sigma^2 t^2}{2}} \cos(\gamma_\mu \langle B_z \rangle t)$$

$$\sigma^2 = \gamma_\mu{}^2 \langle \Delta B_z{}^2 \rangle \qquad \text{Relaxation rate } [\mu s^{-1}]$$

$$\sigma = \gamma_\mu \Phi_0 \sqrt{0.00371}\,\frac{1}{\lambda^2}$$

$$\sigma\ [\mu s^{-1}] = 0.1074 \frac{1}{\lambda\ [\mu m]^2}$$

Gaussian field distribution

$$p(B_z) = \frac{\gamma_\mu}{\sqrt{2\pi}\sigma} e^{-\frac{\gamma_\mu^2 (\langle B_z \rangle - B_z)^2}{2\sigma^2}}$$

$$\frac{\sigma^2}{\gamma_\mu{}^2} = \langle \Delta B_z{}^2 \rangle$$

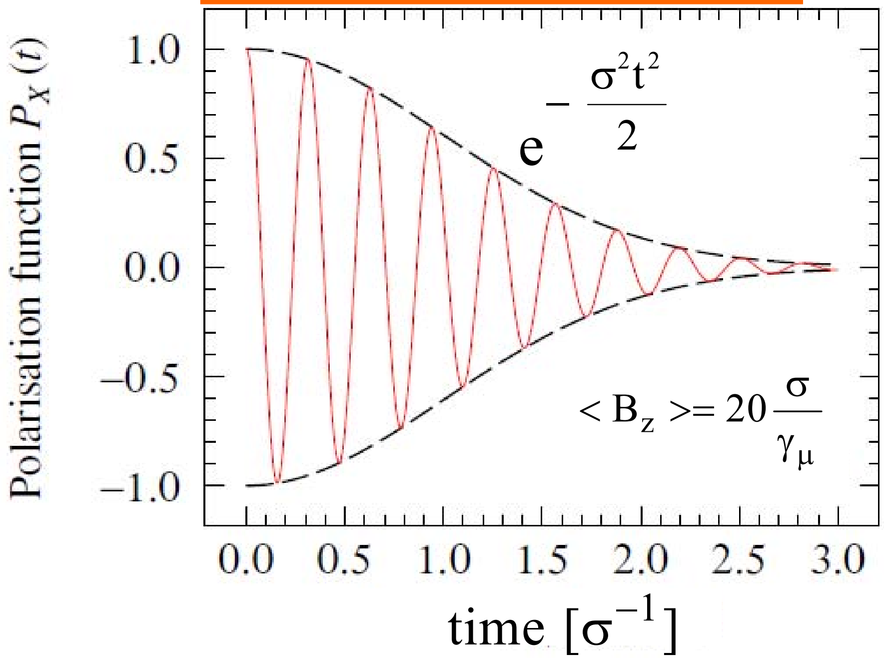

Pümpin et al., Phys. Rev. B 42, 8019 (1990)

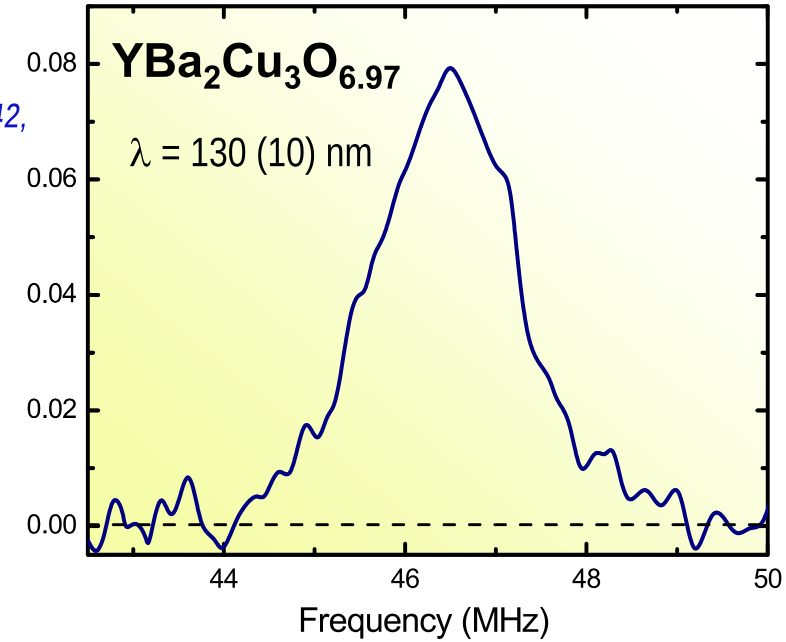

Classification of superconductors

Y.Uemura et al., Phys. Rev. Lett. 66, 2665 (1991)

$$T_c \text{ versus } \sigma \propto \frac{1}{\lambda^2} \propto \frac{n_s}{m^*} \text{ , Uemura plot}$$

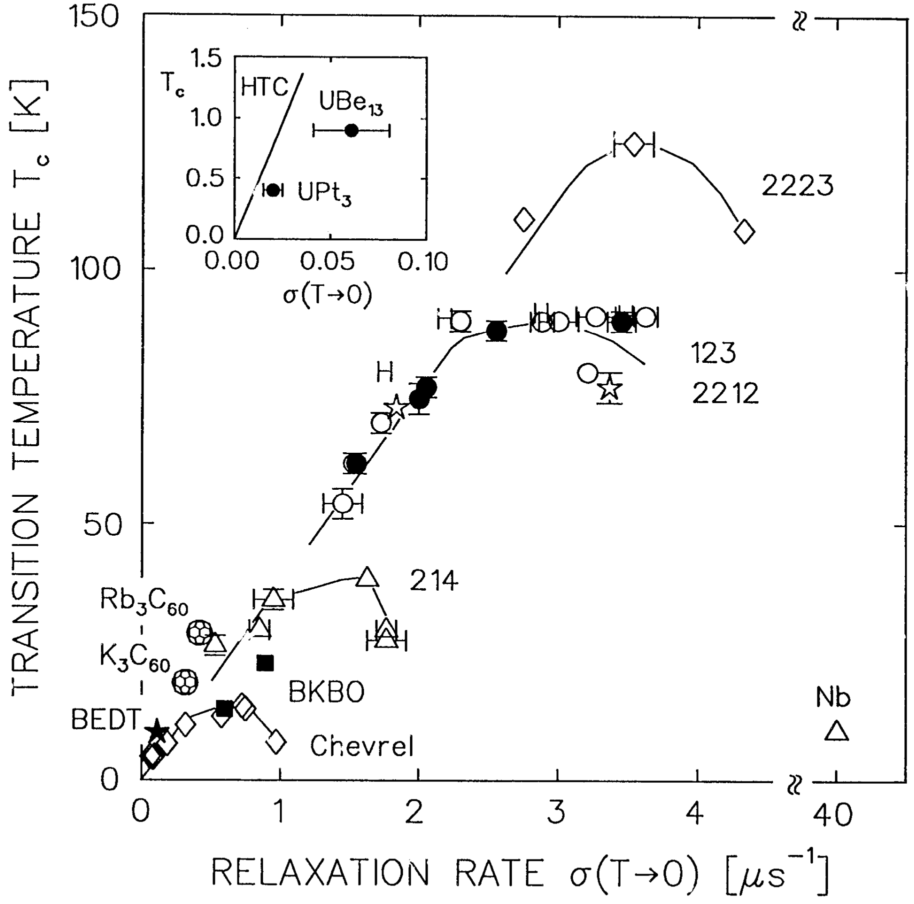

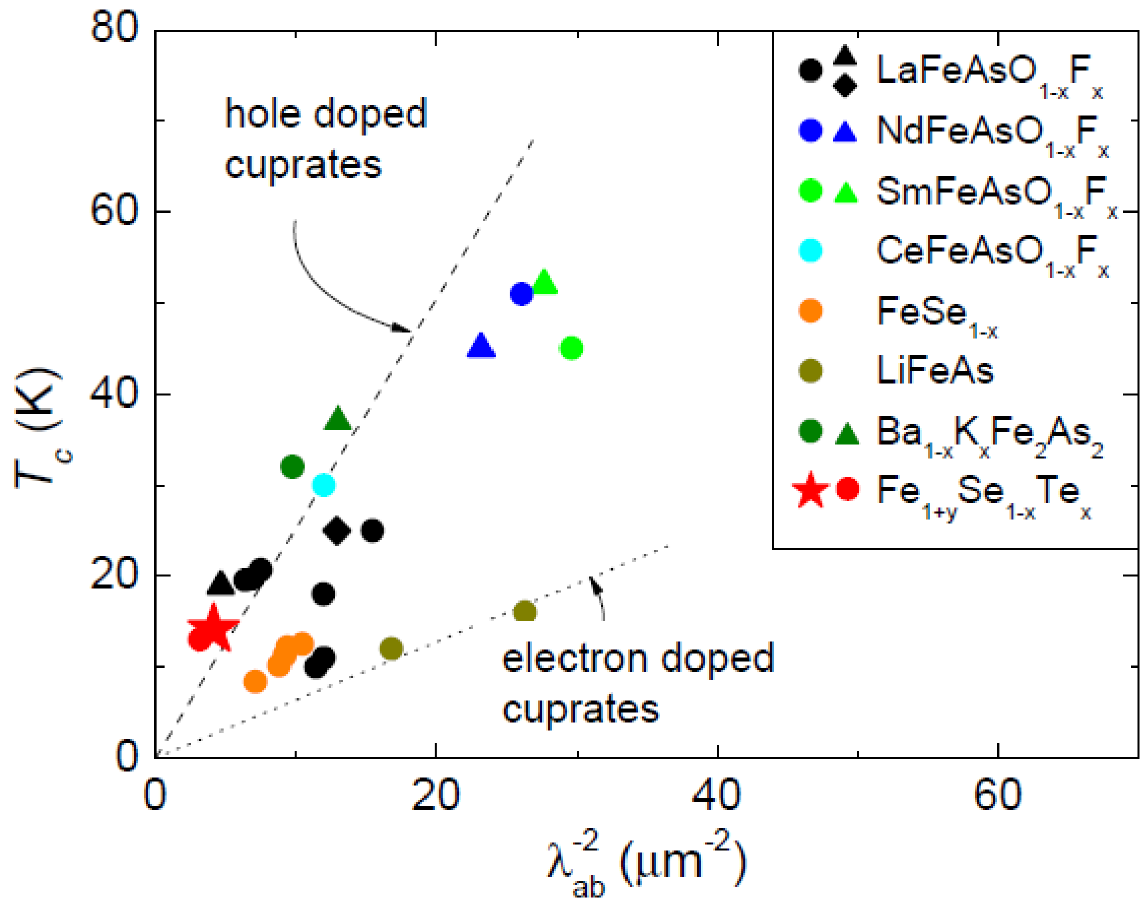

T-dependence of sc carrier density and sc gap

From μSR:

$$\sigma_\mu = \gamma_\mu \sqrt{\langle \Delta B^2 \rangle} \propto \frac{1}{\lambda^2}$$

$$\lambda = \sqrt{\frac{m}{\mu_0 e^2 n_s}}$$

$$\Rightarrow \quad \sigma_\mu \propto \frac{\mu_0 e^2}{m} n_s$$

indications on the SC gap

By taking into account the thermal population of the quasiparticles excitations of the Cooper pairs (Bogoliubov quasiparticles):

$$n_s(T) = n_s(0)\left(1 - \frac{2}{k_B T}\int_0^\infty f(\epsilon,T)\,[1 - f(\epsilon,T)]\,d\epsilon\right)$$

with:

$$f(\epsilon,T) = \left(1 + \exp\left[\sqrt{\epsilon^2 + \Delta(T)^2}/k_B T\right]\right)^{-1}$$

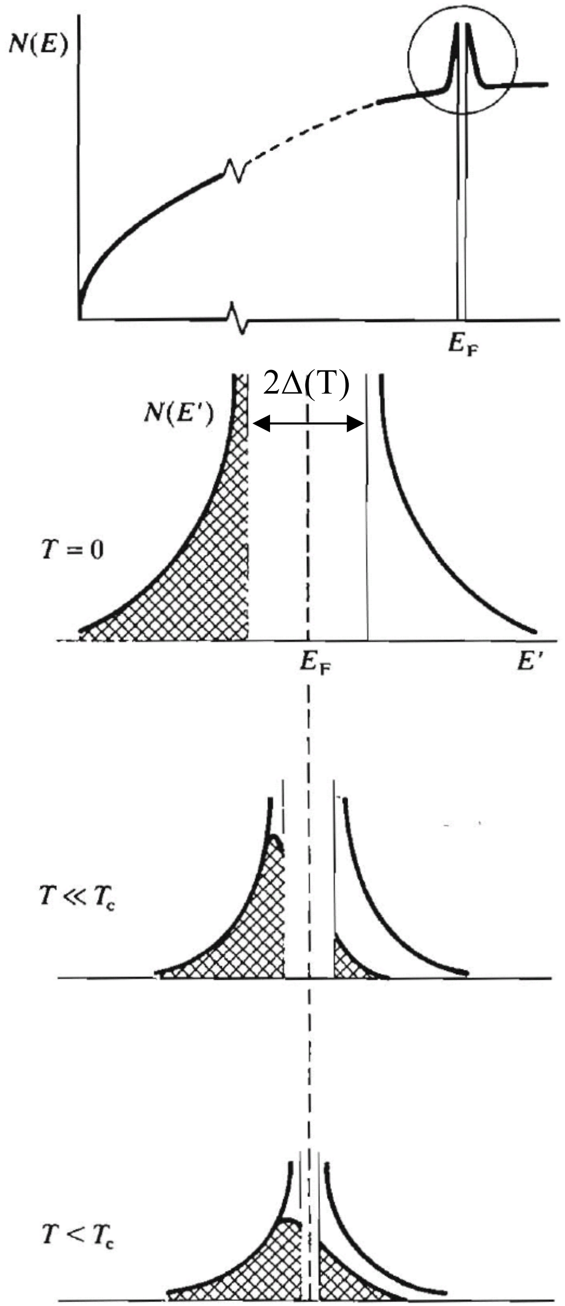

T-dependence of sc carrier density and sc gap

Low temperature dependence of magnetic penetration depth reflects symmetry of superconducting gap function

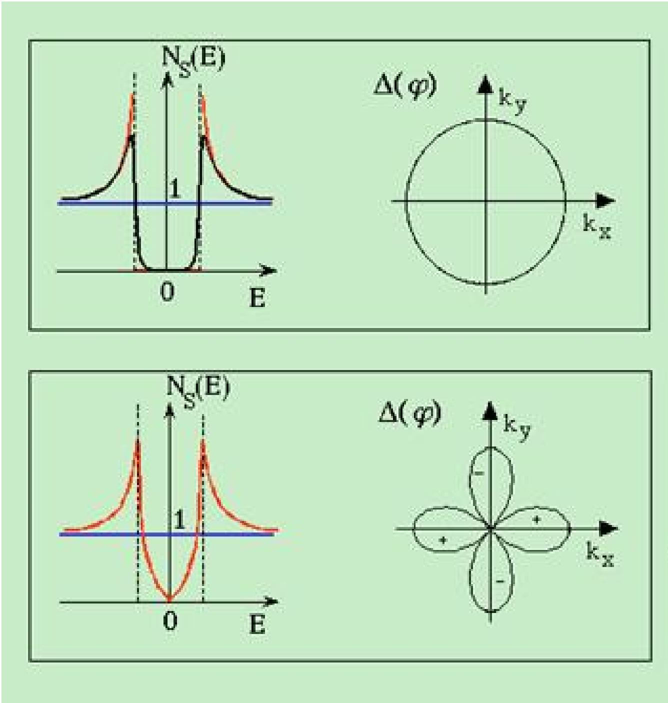

$\mathrm{s-wave\ gap}$

$\Delta(T,\varphi)=\Delta(T)$

$$\lambda(T)=\lambda(0)\left(1+\sqrt{\frac{\pi\Delta(0)}{2k_BT}}\exp\left[-\Delta(0)/k_BT\right]\right)$$

$\mathrm{d-wave\ gap}$

$\Delta(T,\varphi)=\Delta(T)\cos(2\varphi)$

$\tan\varphi=\frac{k_y}{k_x}$

$$\lambda(T)=\lambda(0)\left(1+\frac{\ln 2}{\Delta(0)}T\right)$$

T-dependence of sc carrier density and sc gap

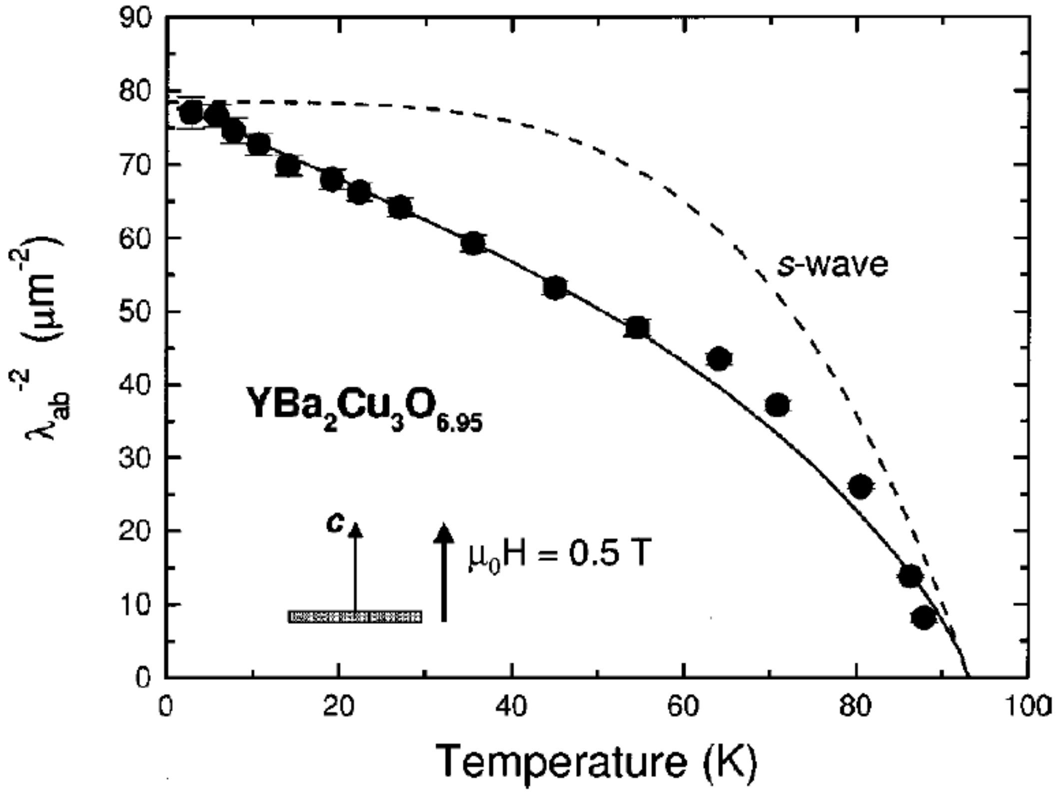

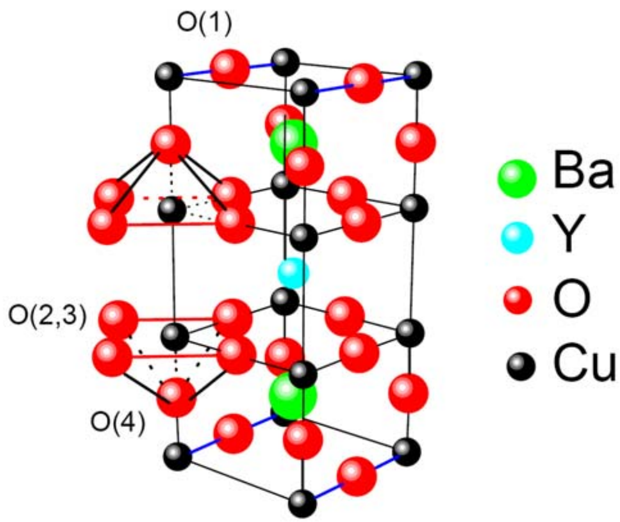

μSR measurement: *J. Sonier et al., Phys. Rev. Lett.,* ***72****, 744 (1994)*

microwave measurement: *W.N. Hardy et al., Phys. Rev. Lett* ***70****, 3999 (1993)*

Phase diagram

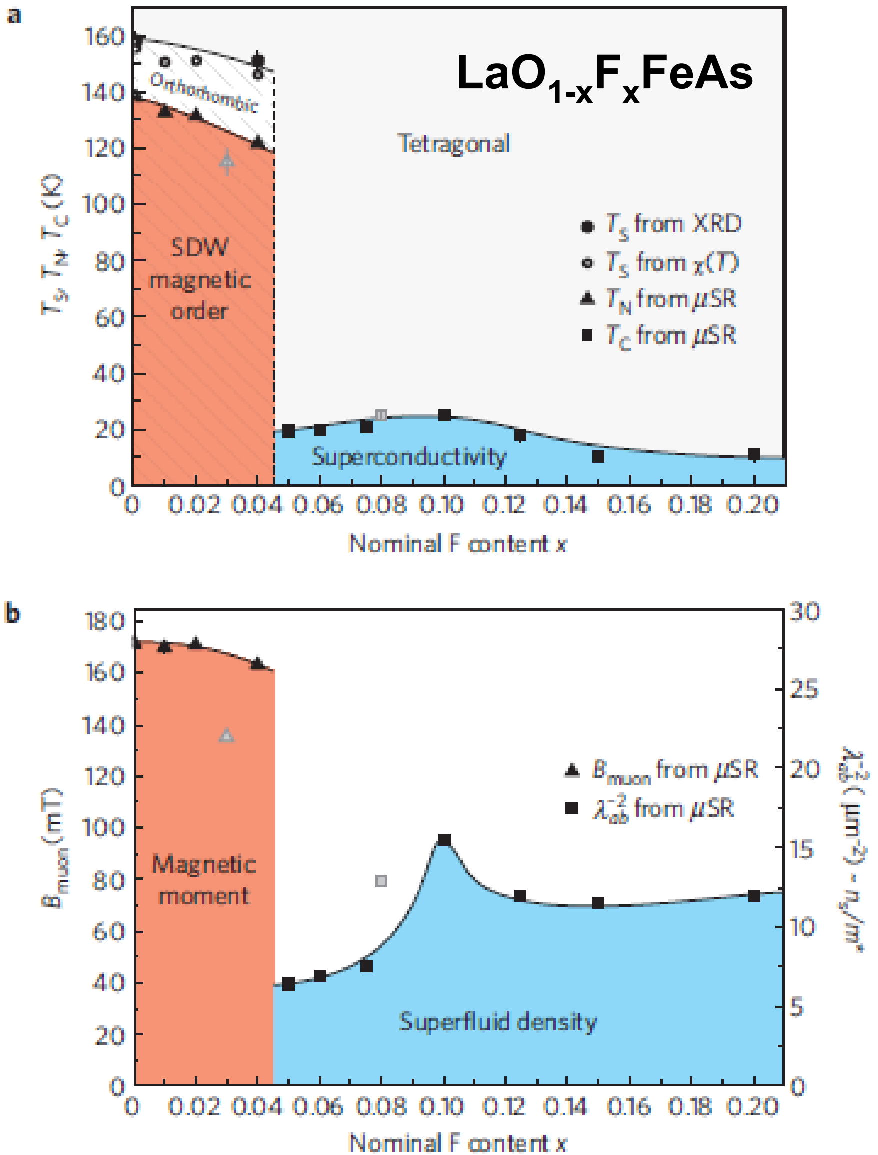

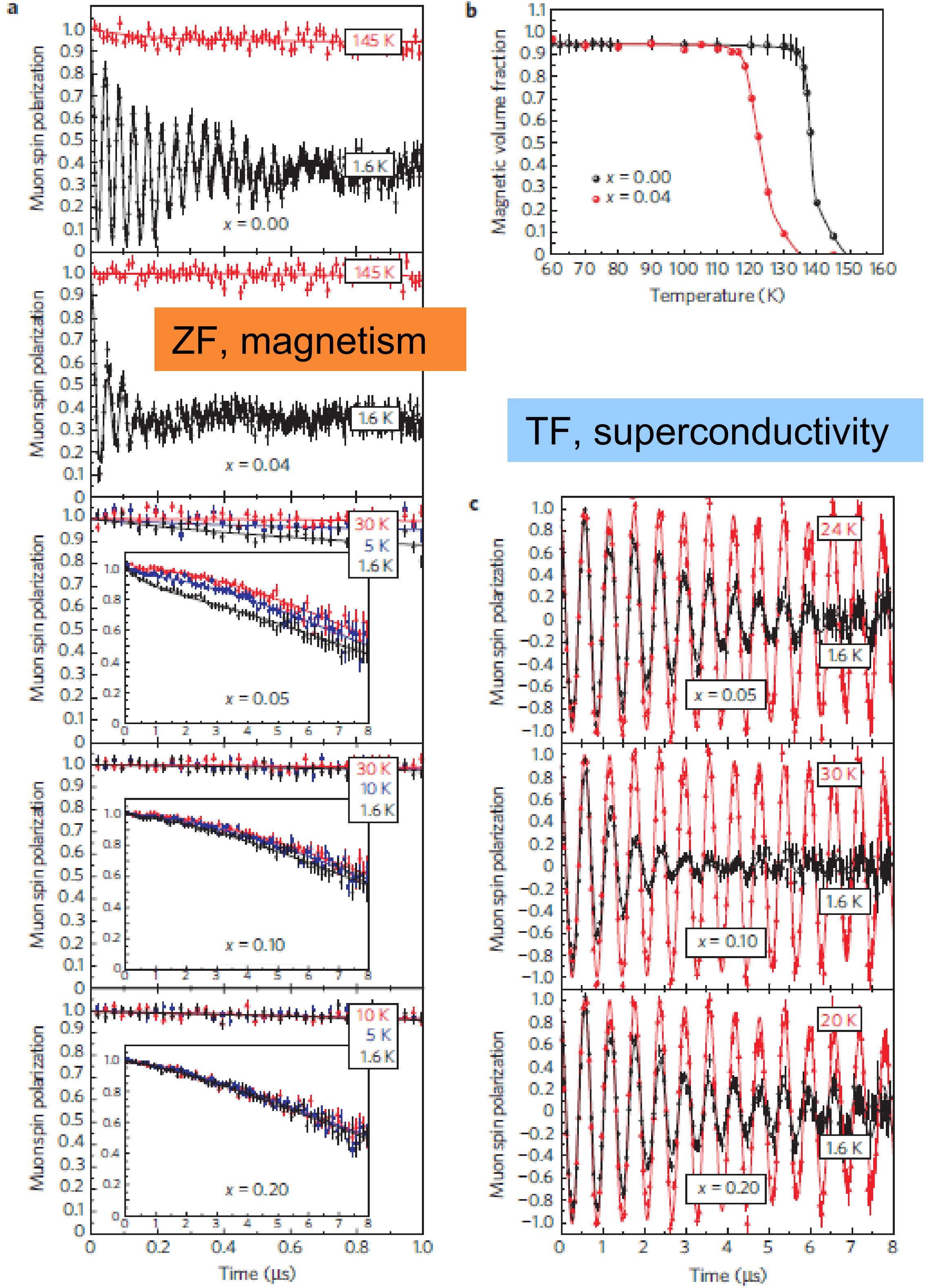

ZF, magnetism

TF, superconductivity

H. Luetkens et al., Nature Materials 8, 305 - 309 (2009)

Coexistence of magnetic and sc order: $YBa_2Cu_3O_{6+x}$

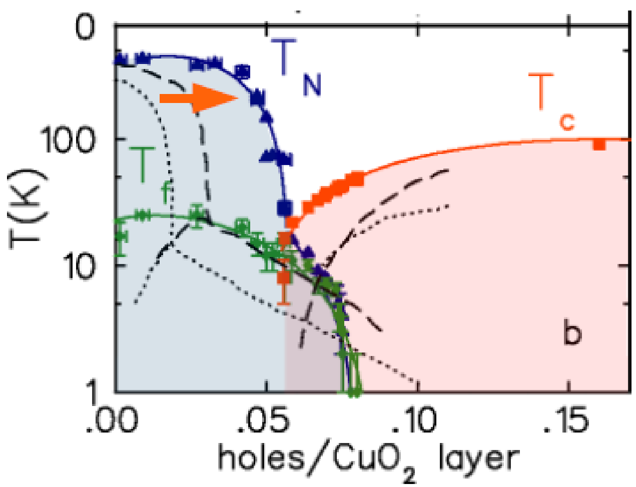

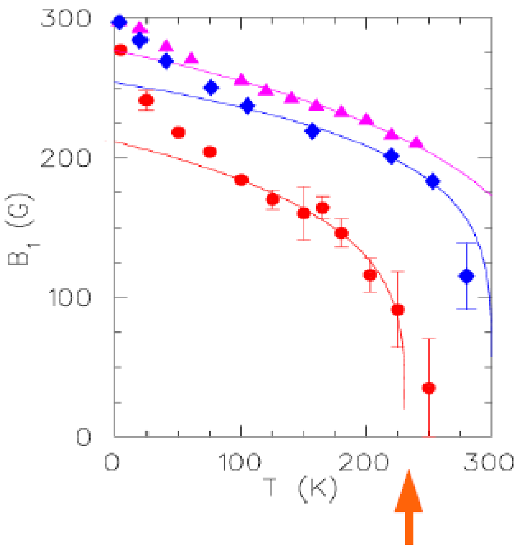

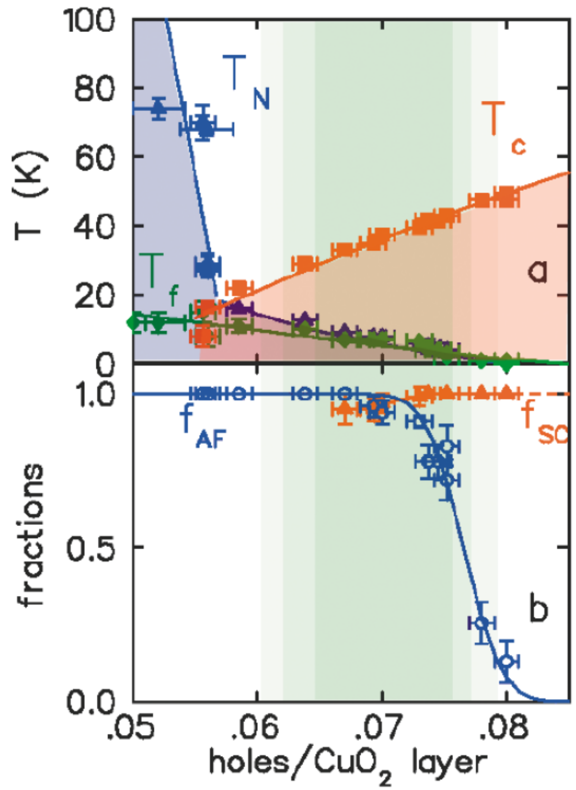

Magnetism from ZF measurements:

$$A_z(t) = a_L G_z(t) + a_T G_x(t)\cos(\gamma_\mu |\vec{B}_1| t)$$

$$a_L + a_T = a_{ZF}$$

$\vec{B}_1$: local field

for a homogeneous magnetic sample:

$$\frac{a_L}{a_{ZF}} = \frac{1}{3} \quad \text{and} \quad \frac{a_T}{a_{ZF}} = \frac{2}{3}$$

if only part of the sample is magnetic

$$\frac{a_L}{a_{ZF}} > \frac{1}{3} \quad \text{and} \quad \frac{a_T}{a_{ZF}} < \frac{2}{3}$$

Magnetic volume fraction:

$$f_{AF} = \frac{3}{2}\frac{a_T}{a_{ZF}} = \frac{3}{2}\left(1 - \frac{a_L}{a_{ZF}}\right)$$

Superconducting volume fraction :

$$f_{SC} = \frac{a_{TF}}{a_0}$$ where a_0 is obtained at $T>T_c$

Superconductivity (vortex state) from TF

$$A_x(t) = a_{TF} e^{-\frac{(\sigma_\mu^2 + \sigma_n^2)t^2}{2}} \cos(\gamma_\mu B_\mu t)$$

$$B_\mu = \mu_0 H(1+\chi) \quad \text{and} \quad \chi < 1$$

S. Sanna et al., Phys. Rev. Lett., ***93*** *207001 (2004)*

Implantation profiles and ranges of muons

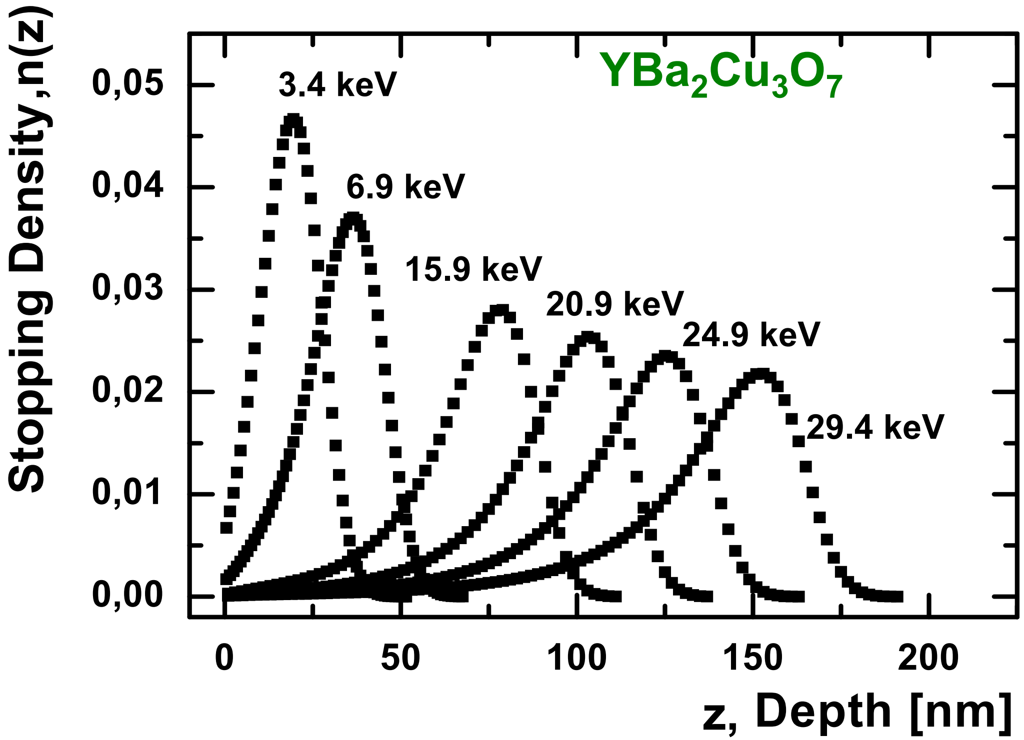

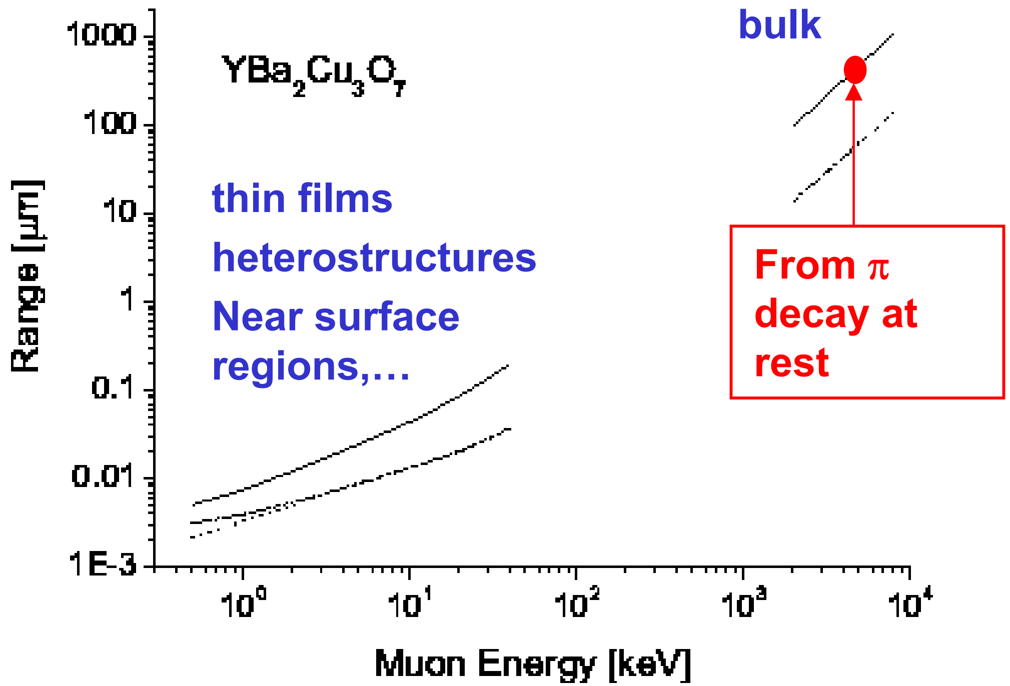

- For thin films studies we need muons with energies in the region of keV rather than MeV
- Tunable energy (E_μ < 30 keV) allows depth-dependent μSR studies (~ 1 – 200 nm)
- Low energy muons are a new magnetic/spin probe for thin films, multilayers, near surface regions, buried layers,..

Stopping profiles calculated with the Monte Carlo code Trim.SP *W. Eckstein, MPI Garching*

Experimentally tested: *E. Morenzoni, H. Glückler, T. Prokscha, R. Khasanov, H. Luetkens, M. Birke, E. M. Forgan, Ch. Niedermayer, M. Pleines, NIM* ***B192****, 254 (2002).*

Generation of polarized epithermal muons by moderation

„Surface“
Muons
~ 4 MeV
~ 100% polarized

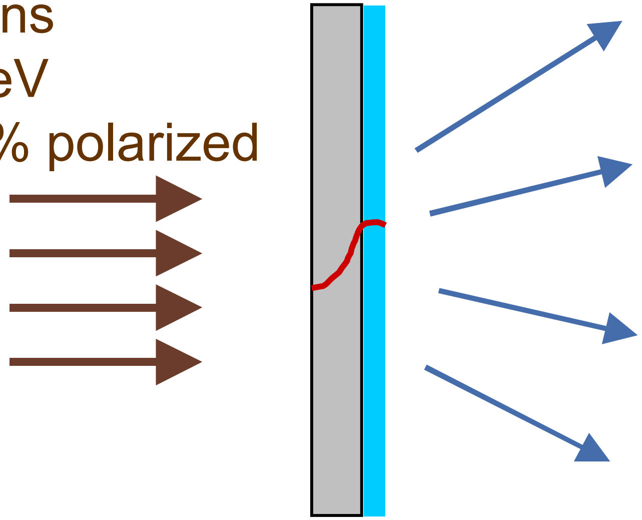

~100 μm Ag
6 K

~ 500 nm
s-Ne, Ar,
s-N_2

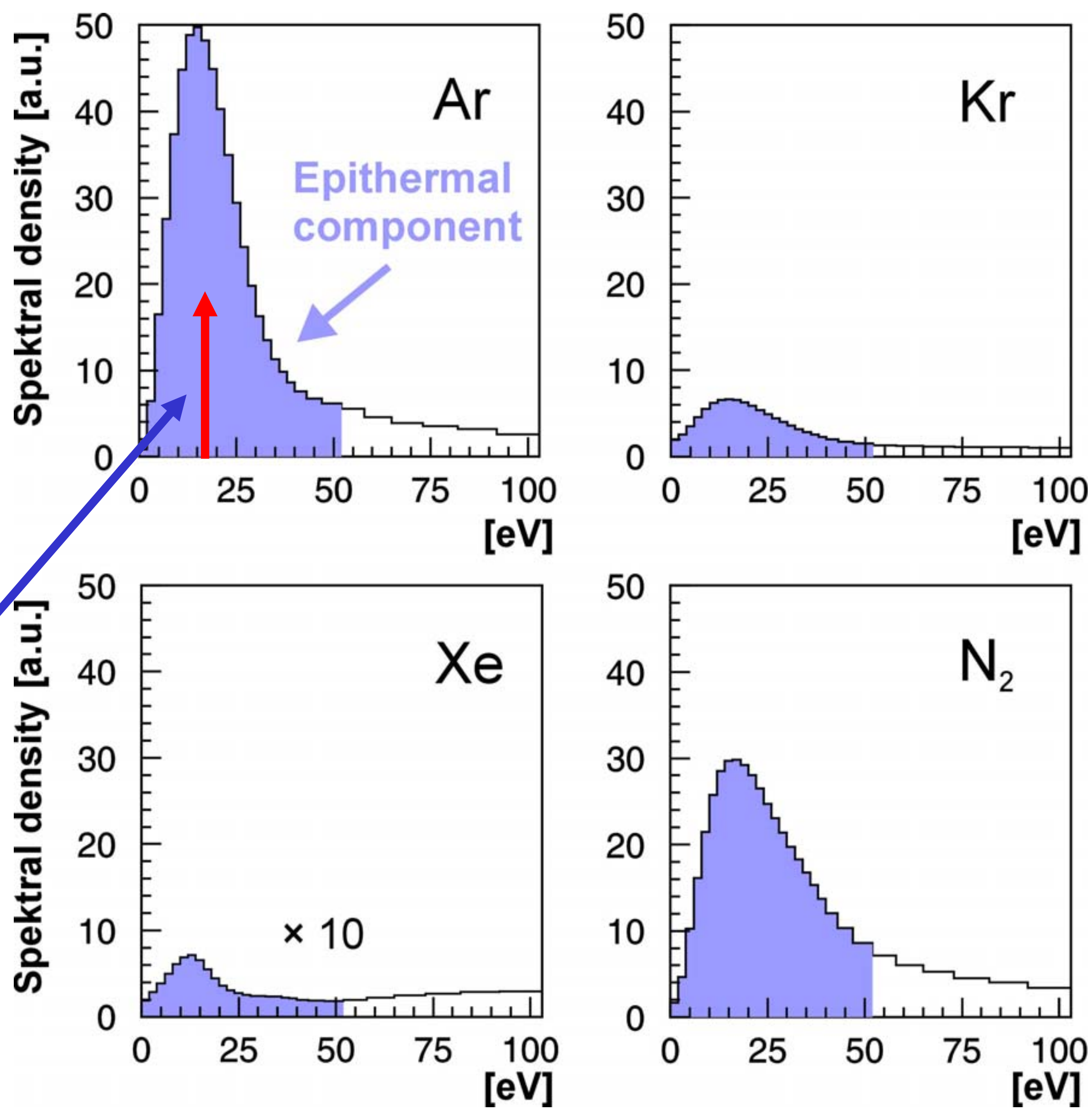

Our source of low energy muons (E ~ 15 eV)

E. Morenzoni et al. J. Appl. Phys. **81**, 3340 (1997).
T. Prokscha et al. Appl. Surf. Sci. (2001)
D. Harshmann et al., Phys. Rev. B36, 8850 (1987).

Characteristics of epithermal muons

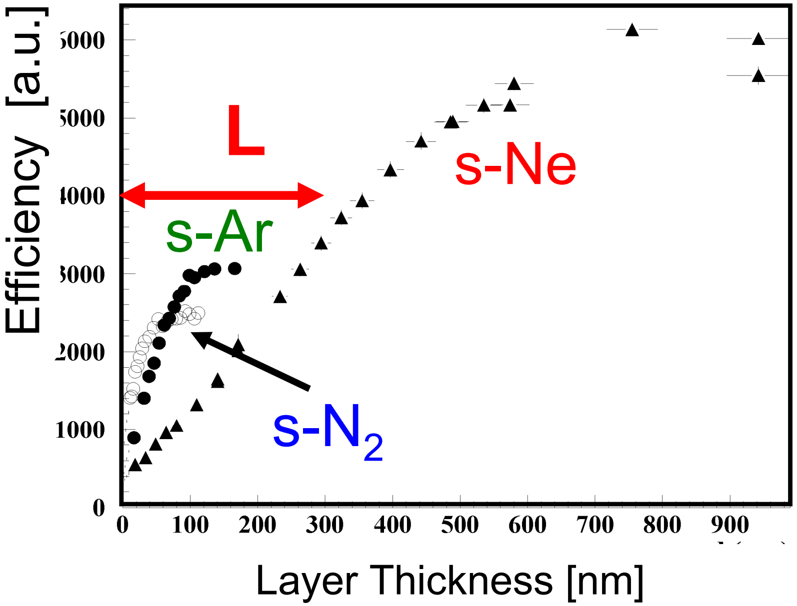

s-Ar: Density of states and band structure

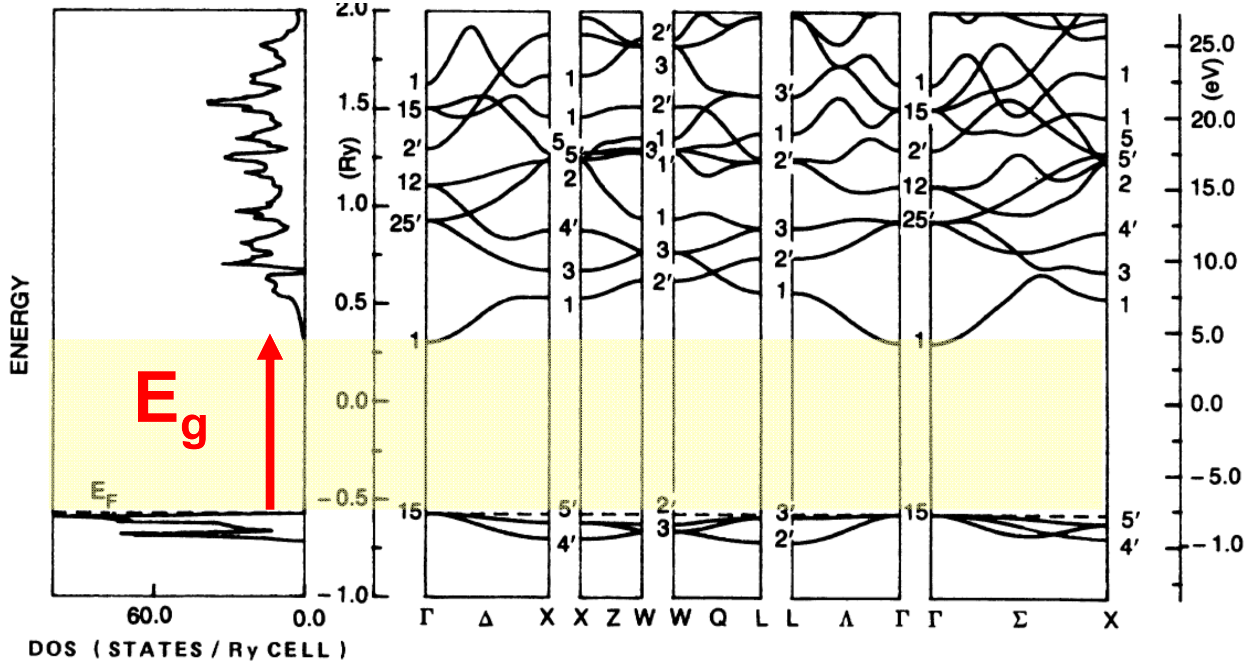

Moderation mechanism:

→ suppression of electronic energy loss for $E_\mu \approx E_g$ (wide band gap insulator)

→ escape before thermalization

→ large escape depth L (50-250 nm)

Moderation efficiency:

$$\varepsilon_{\mu^+} \equiv \frac{N_{epith}}{N_{4MeV}} \cong \frac{(1-F_{Mu})L}{\Delta R} \simeq 10^{-4} - 10^{-5}$$

ΔR: Range width of surface muons $\approx$100 μm

Characteristics of epithermal muons

Polarization of epithermal muons is a necessary condition for their use in μSR

Larmor precession of epithermal muons in an external field.

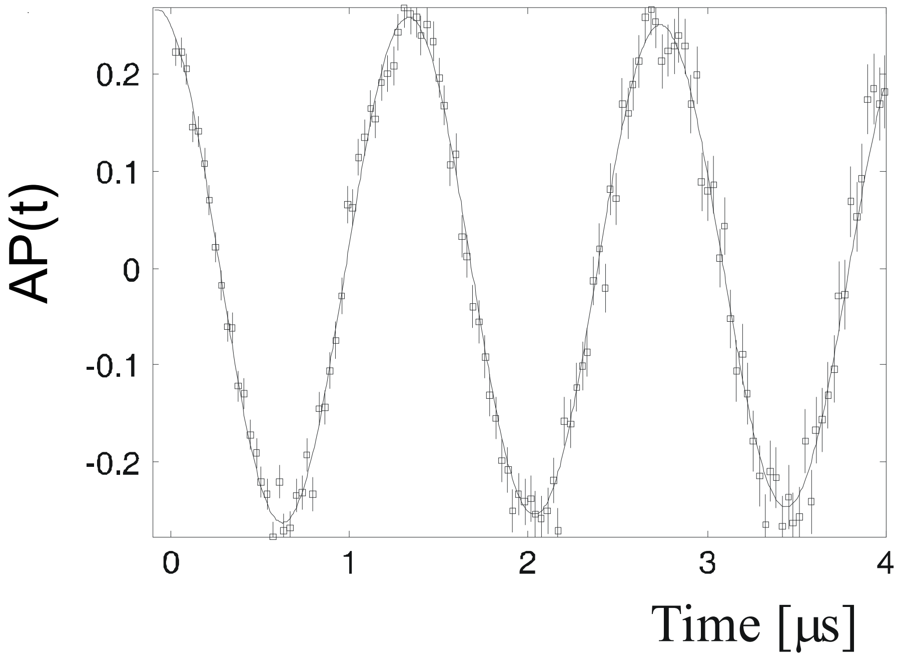

From the amplitude we conclude:

No polarization loss during moderation

(very fast slowing down time: ~10 ps, no depolarizing mechanism that fast)

→ **P(0) ≅1**

E. Morenzoni, F. Kottmann, D. Maden, B. Matthias, M. Meyberg, Th. Prokscha, Th. Wutzke, U. Zimmermann, Phys.Rev.Lett. **72**, 2793 (1994).

Low energy μ^+ beam and set-up for LE-μSR

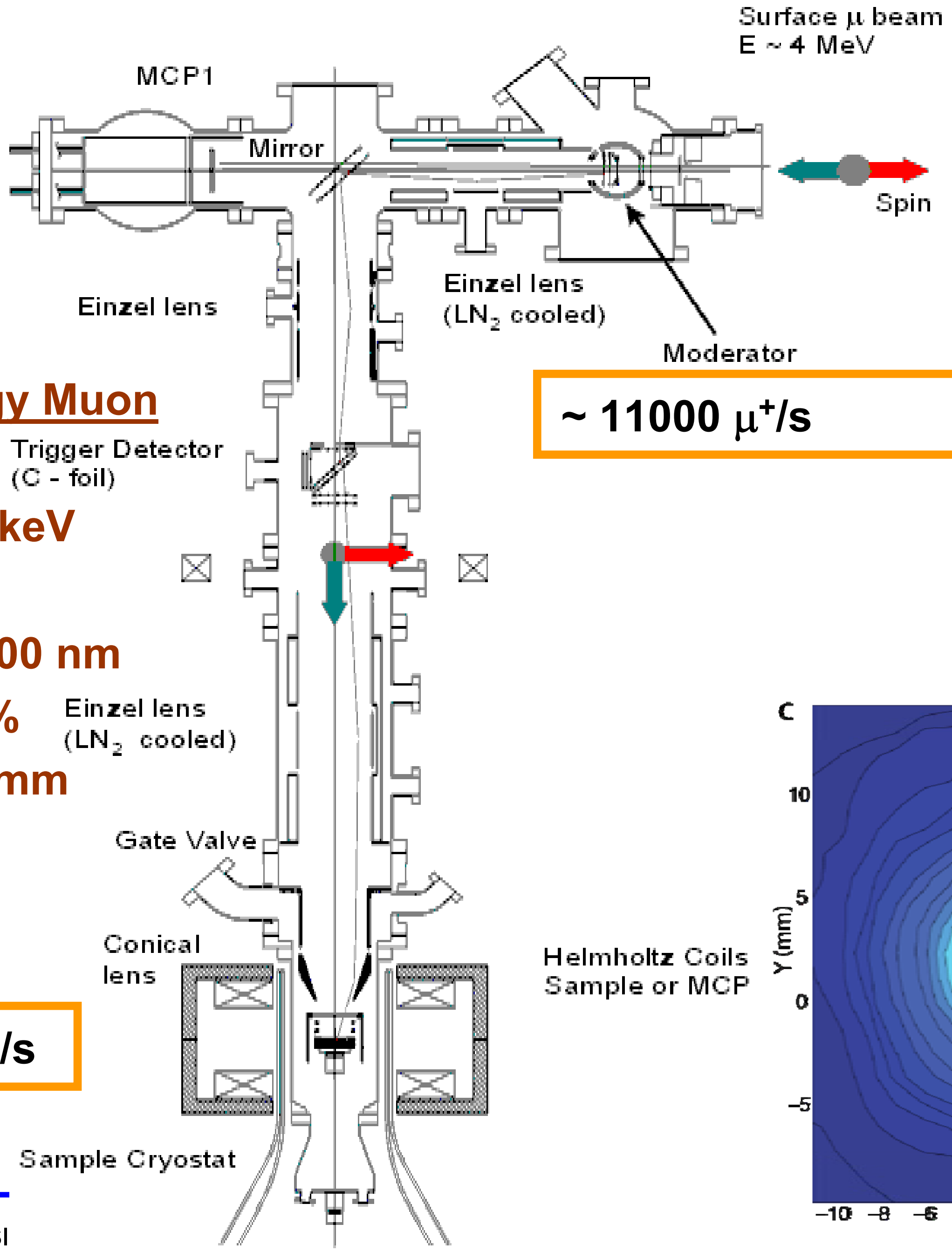

~1.9 •10^8 μ^+/s

from new μE4 beam line

- **UHV system (~10^{-10} mbar)**
- **Electrostatic transport, focussing and energy selection.**
- **All transport elements LN_2 cooled**

~ 11000 μ^+/s

Polarized Low Energy Muon Beam

Energy:	**0.5-30 keV**
ΔE:	**400 eV**
Depth:	**~ 1 – 200 nm**
Polarization	**~ 100 %**
Beam Spot:	**10-20 mm**

~ 4500 μ^+/s

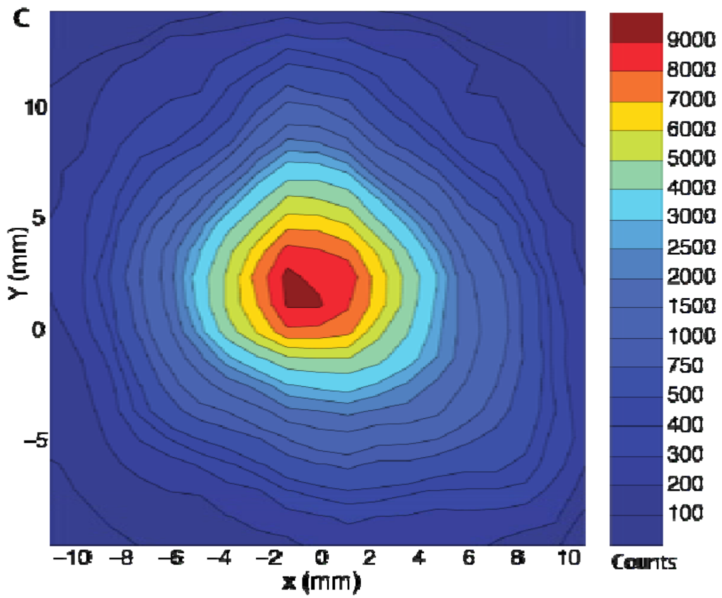

Thin film in the Meissner State

- B_{ext} ($< B_{c1}$) || surface, $T<T_c$ → B=0 in the bulk, but not at the surface

- If $\lambda \gg \xi$ electrodynamic response described by London equations:

1) $\frac{d\vec{j}}{dt} = \frac{1}{\mu_0 \lambda_L^2}\vec{E}$ 2) $\mathrm{rot}\,\vec{j} = -\frac{1}{\mu_0 \lambda_L^2}\vec{B}$ $\left(\vec{j} = -\frac{1}{\mu_0 \lambda_L^2}\vec{A}\right)$

From 2), $\mathrm{rot}\vec{B} = \mu_0 \vec{j}$ and $\mathrm{rot}(\mathrm{rot}\vec{B})$ = grad div$\vec{B}$ - $\Delta\vec{B}$ it follows

$$\Delta\vec{B} = \frac{1}{\lambda_L^2}\vec{B}$$

which in the thin film geometry $\vec{B}_{ext} \parallel \hat{x}$ gives

$B(z) = B_{ext} e^{-\frac{z}{\lambda_L}}$ $\rightarrow \lambda(T) = \sqrt{\frac{m^*}{\mu_0 e^2 n_s(T)}}$ (clean limit $\ell \gg \xi_0$)

λ_L magnetic penetration depth (London)

m^*, n_S effective mass and density of superconducting carriers

F. and H. London,
Proc. Roy. Soc. A149, 71 (1935)

Depth dependent μSR measurements

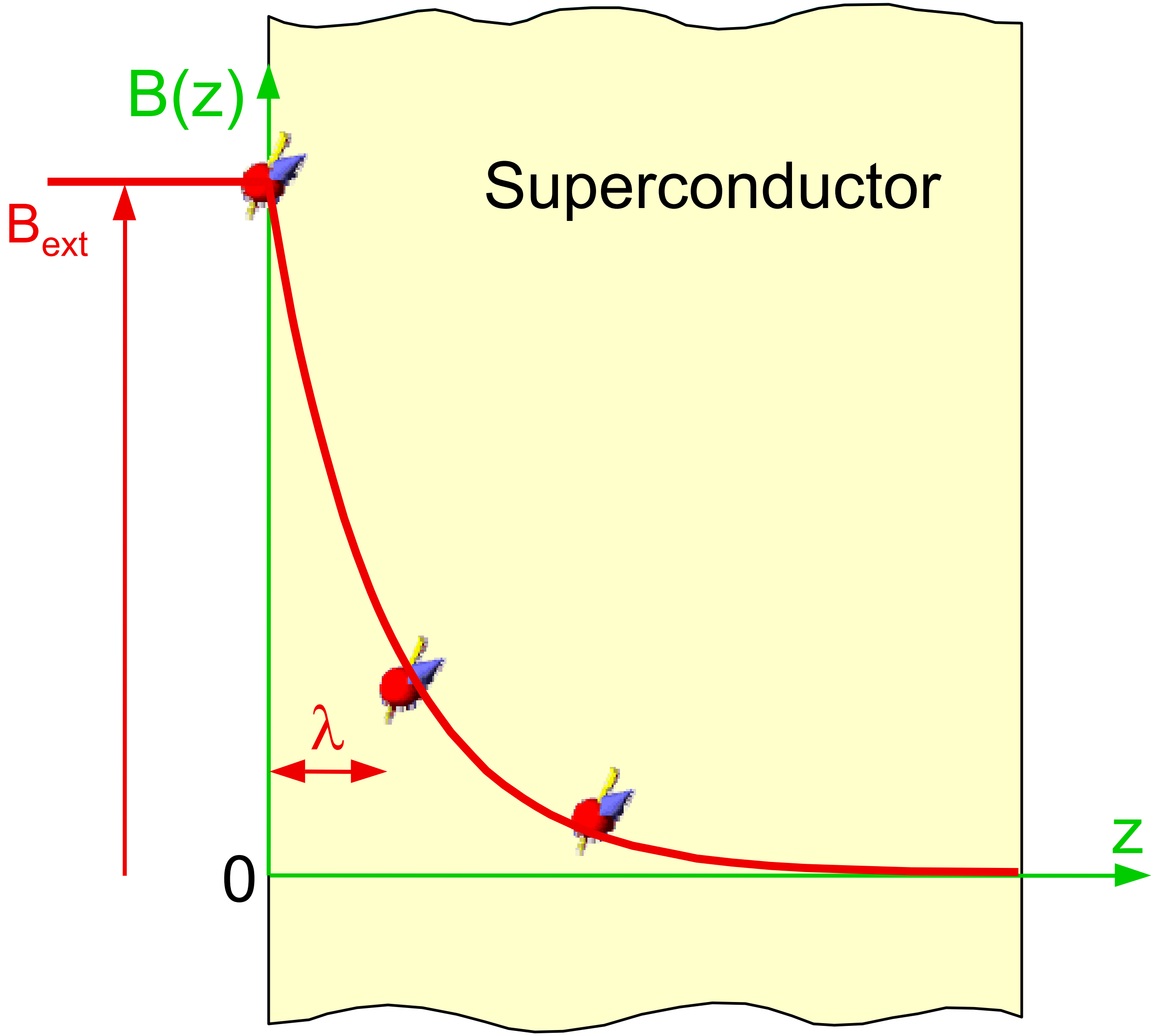

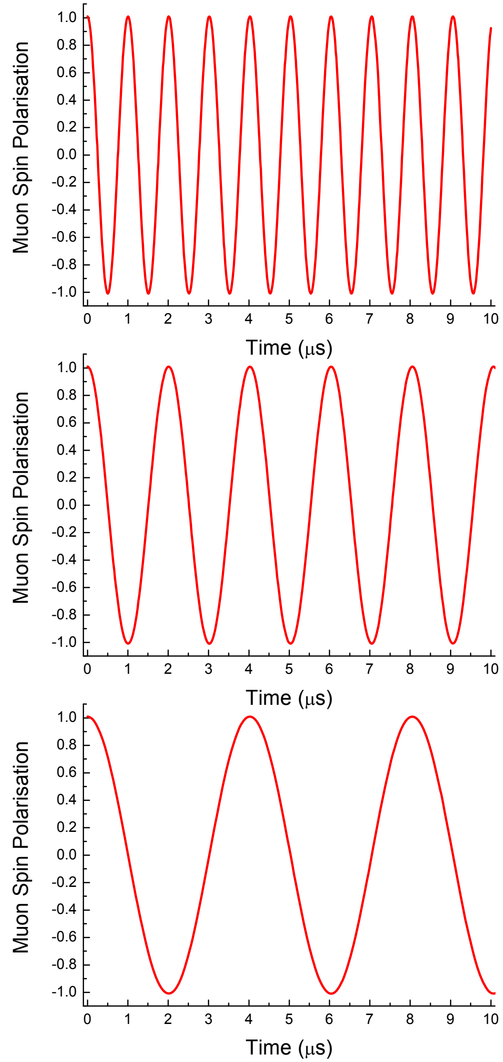

$$\omega_{\mu}(z) = \gamma_{\mu} B_{loc}(z)$$

<B> vs <z> ⇒ B(z)

→ Magnetic field profile B(z) over nm scale

→ Characteristic lengths of the sc λ, ξ

More precise: use known implantation profiles

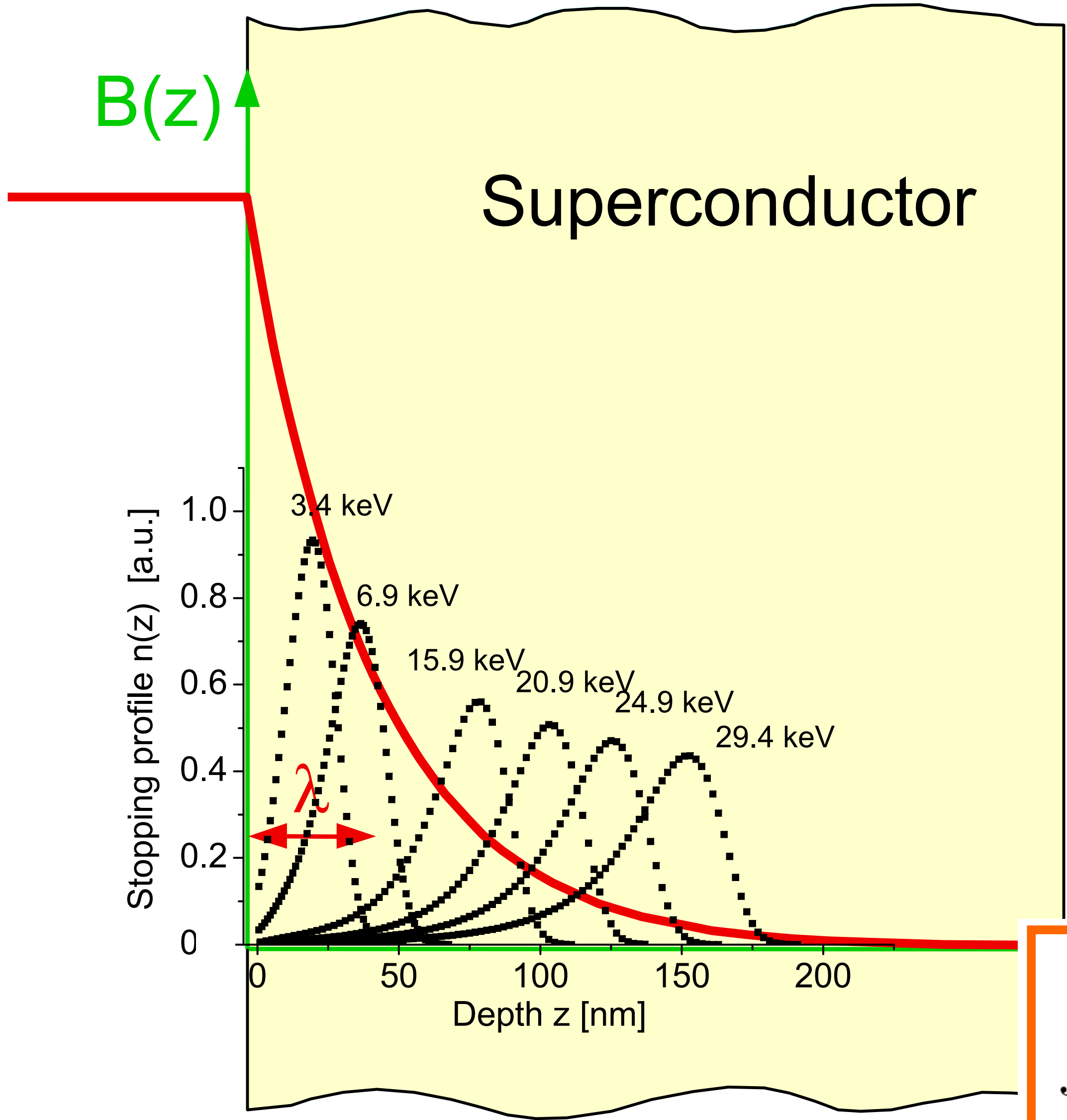

n(z,E): muon implantation profile for a particular muon energy E

μSR experiment ⇒ magnetic field probability distribution p(B, E) sensed by the muons

$$n(z, E)\,\mathrm{d}z = p(B, E)\,\mathrm{d}B$$

$$\int_0^z n(\zeta, E)\,\mathrm{d}\zeta = \int_{B(z)}^{\infty} p(\beta, E)\,\mathrm{d}\beta$$

⇒ B(z)

→ Magnetic field profile B(z) over nm scale

→ Characteristic lengths of the sc λ, ξ

In plane anisotropy λ_a , λ_b in detwinned $YBa_2Cu_3O_{6.95}$

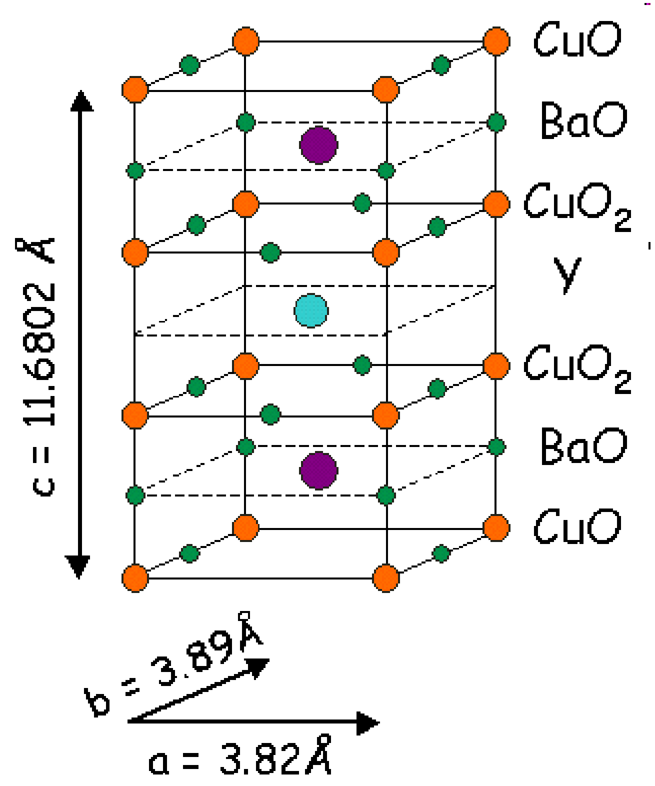

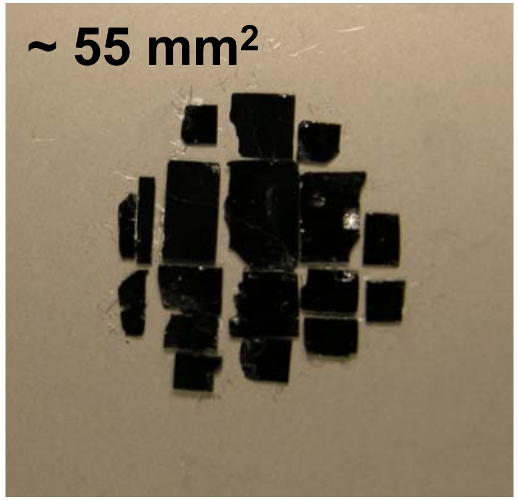

Detwinned (>95%) $YBa_2Cu_3O_{6.95}$ crystals optimally doped
(T_c= 94.1 K, $\Delta T_c \leq$ 0.1K)

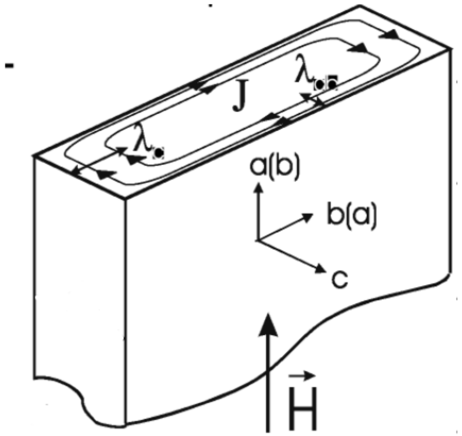

$$\vec{H}_{ext} \parallel \hat{a}\text{-axis} \rightarrow \lambda_b$$
$$\vec{H}_{ext} \parallel \hat{b}\text{-axis} \rightarrow \lambda_a$$

samples produced by R. Liang, W. Hardy, D. Bonn, Univ. of British Columbia

$\vec{B}_{ext} = 9.47\text{mT} \quad \| \ \hat{a}\text{-axis}$

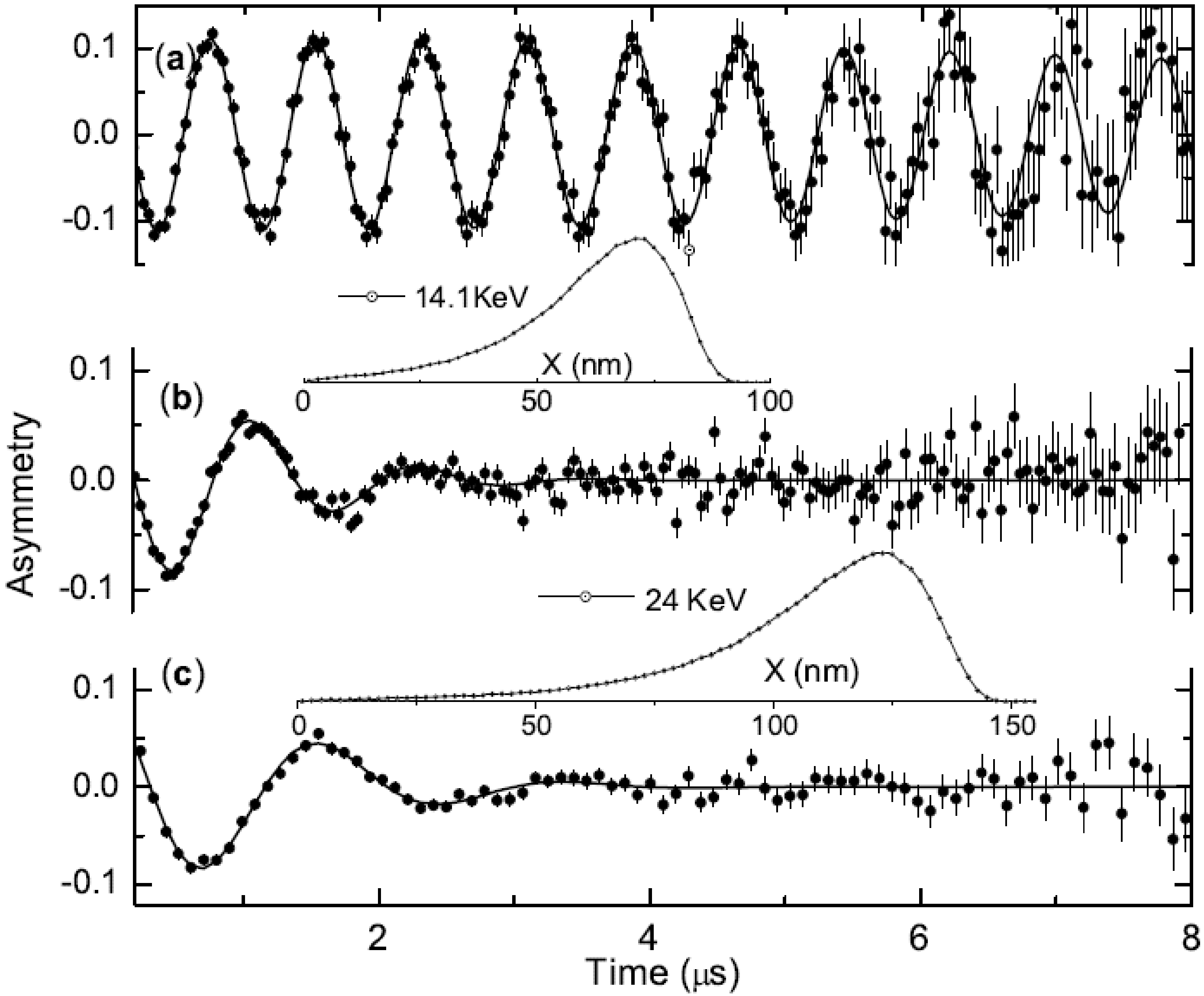

T = 110 K

T = 8 K

$\vec{B}_{ext} = 9.47\text{mT}$, T=8 K

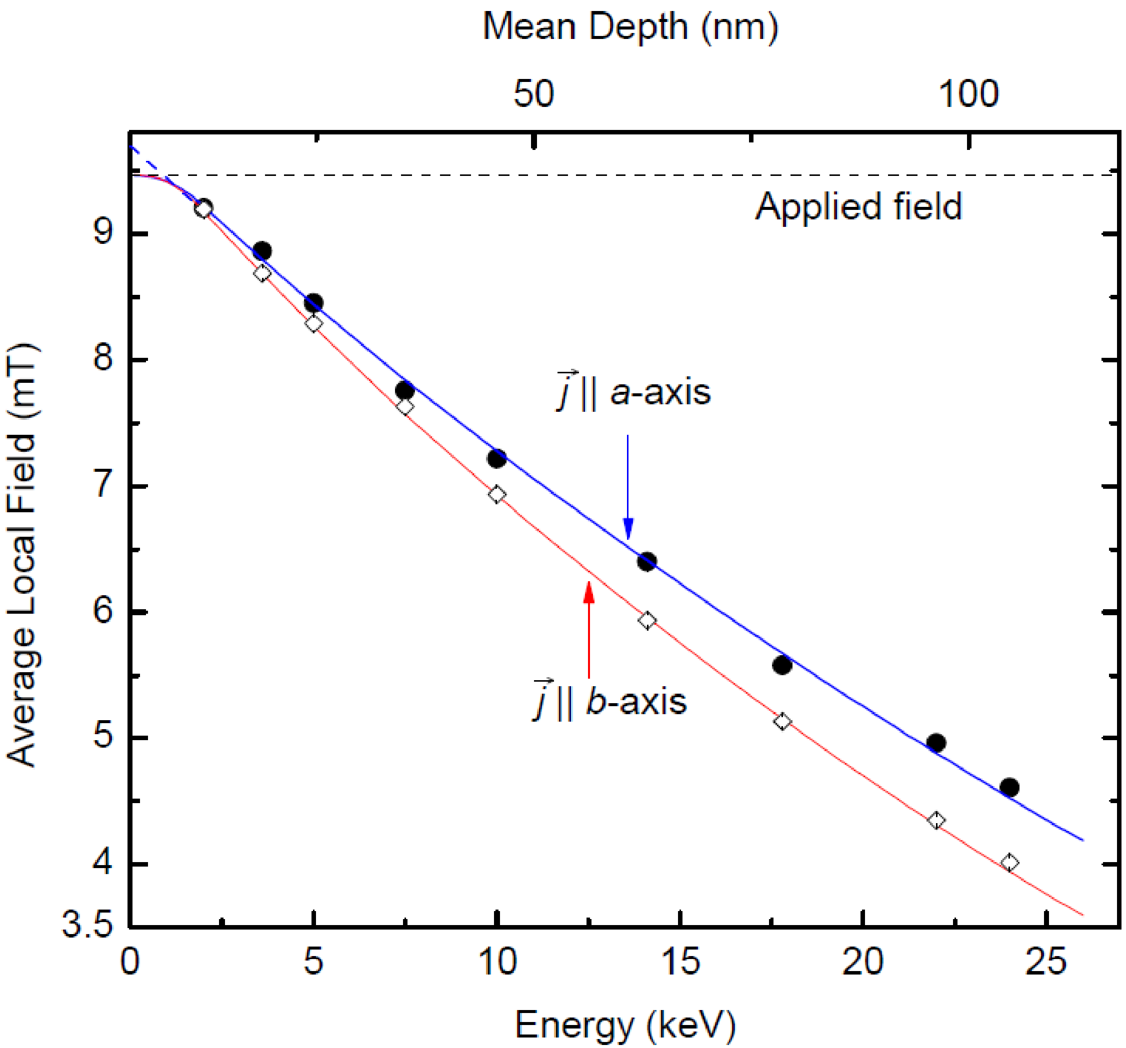

$$B(z) = \begin{cases} B_0 \exp\left[-(z-d)/\lambda_{a,b}\right] & , z \geqslant d \\ B_0 & , z < d \, , \end{cases}$$

$$d = 10.3(4) \ \text{nm}$$

$$\mathcal{A}(t) = A \exp\left[-\sigma^2 t^2/2\right] \int \rho(z) \cos\left[\gamma_\mu B(z) t + \phi\right] \, dz$$

d-wave superconductor

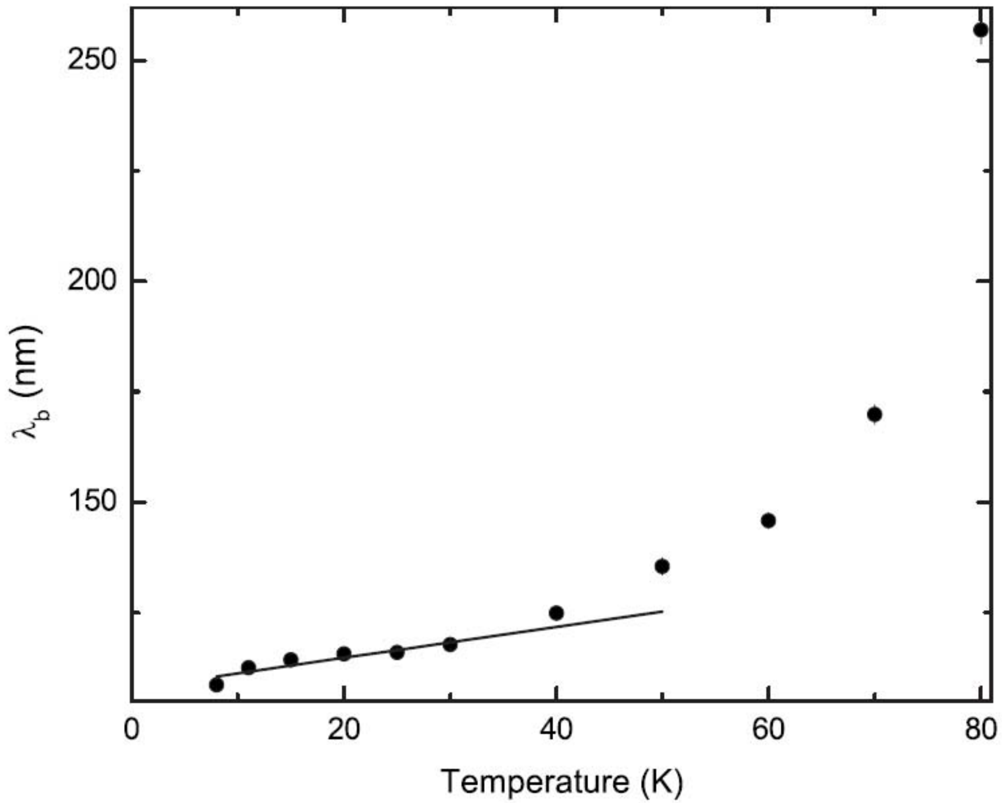

FIG. 3. Temperature dependence of the London penetration depth in an external magnetic field of 9.46 mT applied parallel to the *a* axis so that the shielding currents are in the *b* direction and parallel to the CuO chains.

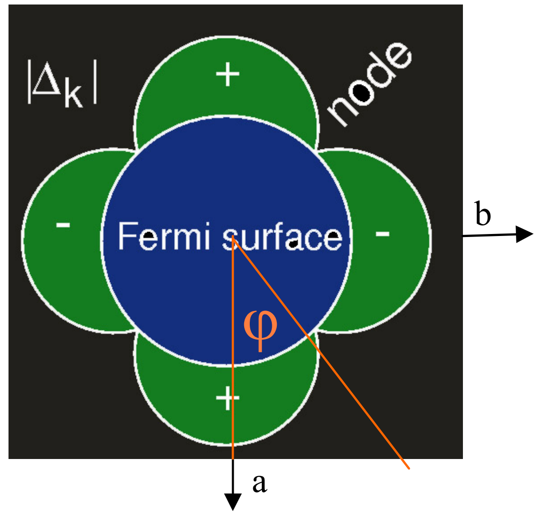

for $\Delta=\Delta(0)\cos(2\varphi)$

for low T:

$$\lambda(T) \cong \lambda(0)\left(1+\frac{\ln 2k_B T}{\Delta(0)}\right)$$

$$\frac{\Delta\lambda}{T} = 0.35(7)\frac{\text{nm}}{\text{K}}$$

λ_a= 126 ± 1.2 nm, λ_b=105.5 ± 1.0 nm , λ_{ab}= 115.3 ± 0.8 nm, λ_a/λ_b=1.19 ± 0.01

*R.F. Kiefl et al. , Phys. Rev. B **81**, 180502R (2010)*

Magnetic multilayers (ML)

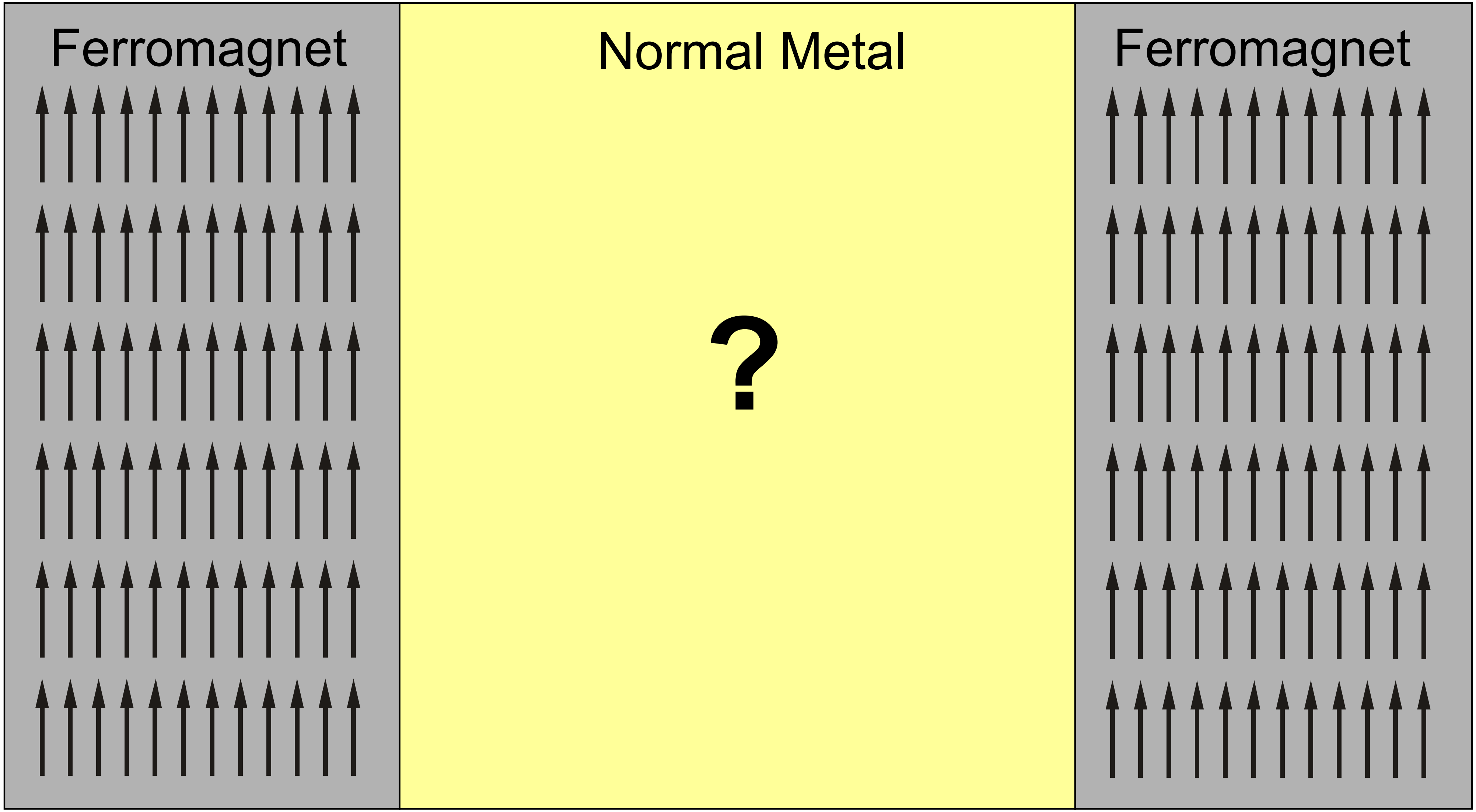

Interlayer exchange coupling in magnetic ML

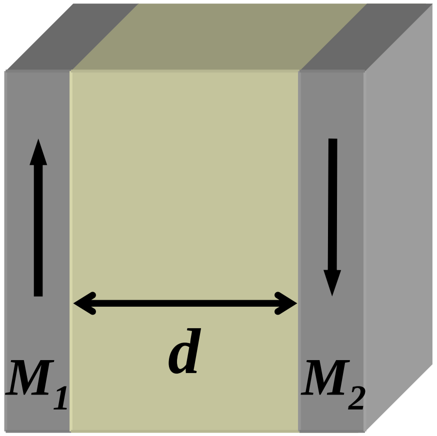

$$\mathcal{H}_{\mathrm{IEC}} = -J(d)\, \boldsymbol{M_1} \cdot \boldsymbol{M_2}$$

IEC in trilayers with non-magnetic spacer:
Example: Co/Cu/Co

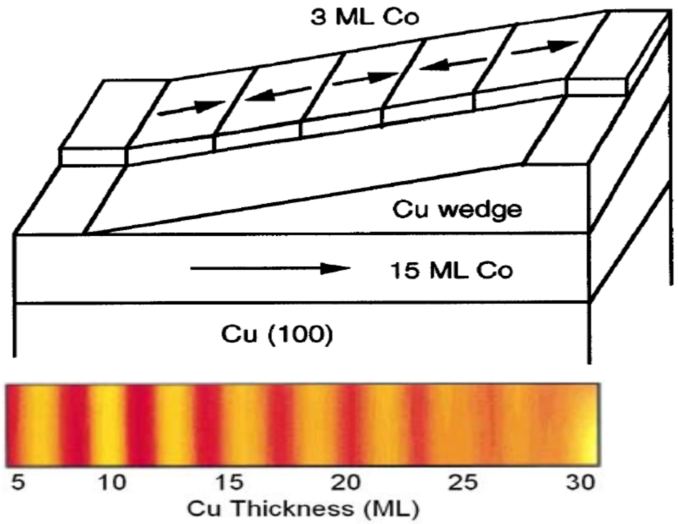

- IEC oscillates with spacer thickness (Model: RKKY)

$$J(d) \propto \frac{1}{d^2} \cos(qd + \phi)$$

- Different techniques to probe the FM layer (polarization of secondary electrons, MOKE, …)
  → oscillation period, coupling strength

- Muons can probe the spatially varying polarization of the nonmagnetic spacer (Spin Density Wave) mediating the coupling between the FM layers.

RKKY Model

Interaction between two moments via conduction electrons

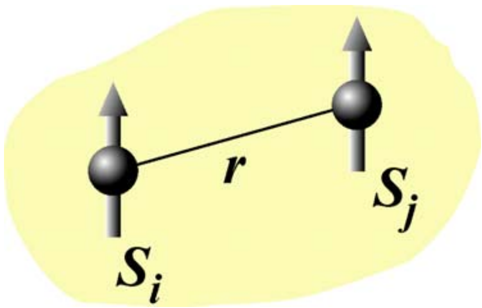

$$\mathcal{H}_{\mathrm{RKKY}} = -J(r)\ \boldsymbol{S_i} \cdot \boldsymbol{S_j}$$

$$J(r) \propto \frac{1}{r^3} \cos(2k_F r + \phi)$$ (leading term for spherical FS)

Interaction between two layers: Integrate over interfaces

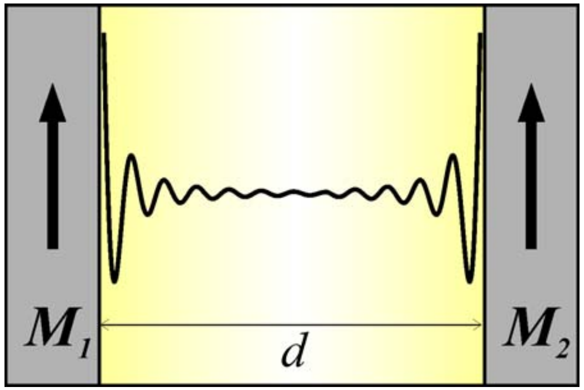

$$J(d) \propto \frac{1}{d^2} \cos(qd + \phi)$$

$$E = -J(d)\ \boldsymbol{M_1} \cdot \boldsymbol{M_2}$$

In non-spherical Fermi surfaces, oscillations of IEC determined by critical spanning vectors

P. Bruno, C. Chappert, Phys. Rev. Lett. ***67****, 1602 (1991)*

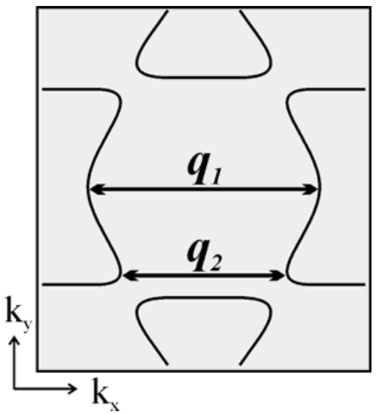

→ $$J(d) \propto \sum \frac{1}{d^{p_i}} \cos(q_i d + \phi) \qquad p_i \leq 2$$

critical spanning vectors Ag: $\lambda_1^{eff} = 11.8\ \text{Å},\ \lambda_2^{eff} = 4.7\ \text{Å}$

Oscillating polarization of conduction electrons

Critical spanning vectors in Ag:

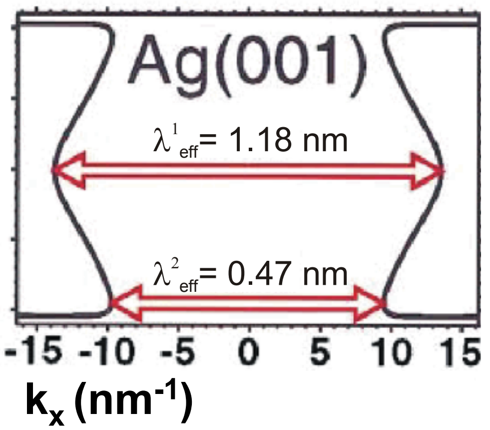

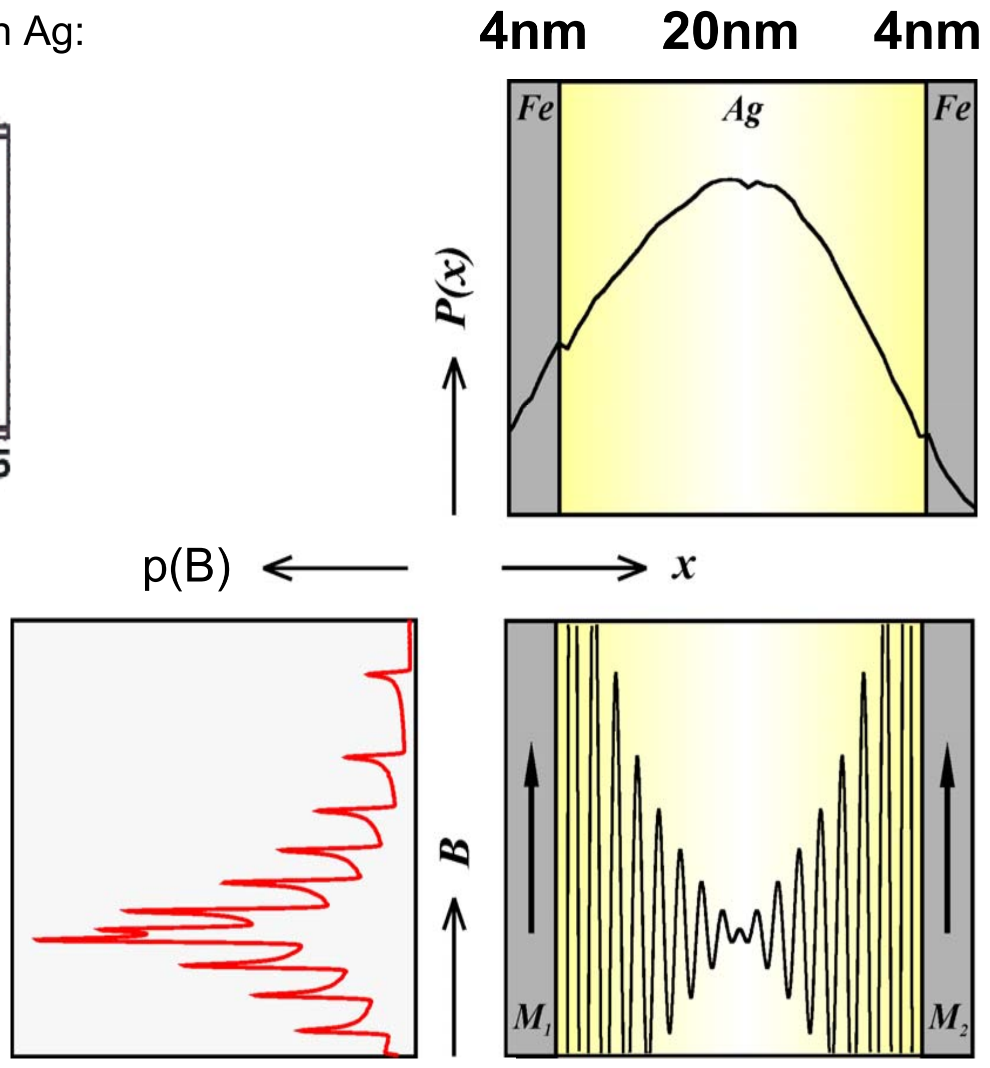

$P(x) \propto B(x)$

Fe/Ag/Fe

Implantation profile of 3 keV muons.

We expect an oscillating spin polarization of conduction electrons P(x) in Ag

→ The depth resolution of LE-μSR cannot resolve the oscillations (WL ~ 1 nm or less), but the oscillating behavior if present is reflected in the field distribution p(B) sensed by the muons. Turning points of oscillations should produce side bands to the B_{ext}.

H. Luetkens, J. Korecki, E. Morenzoni, T. Prokscha, M. Birke, H. Glückler, R. Khasanov, H.-H. Klauss, T. Slezak, A. Suter, E. M. Forgan, Ch. Niedermayer, and F. J. Litterst Phys Rev. Lett. **91**, 017204 (2003).

Oscillating polarization of conduction electrons

This is what is observed in the field distribution obtained by Maximum Entropy Fourier analysis.

Magnetic field distribution in Ag

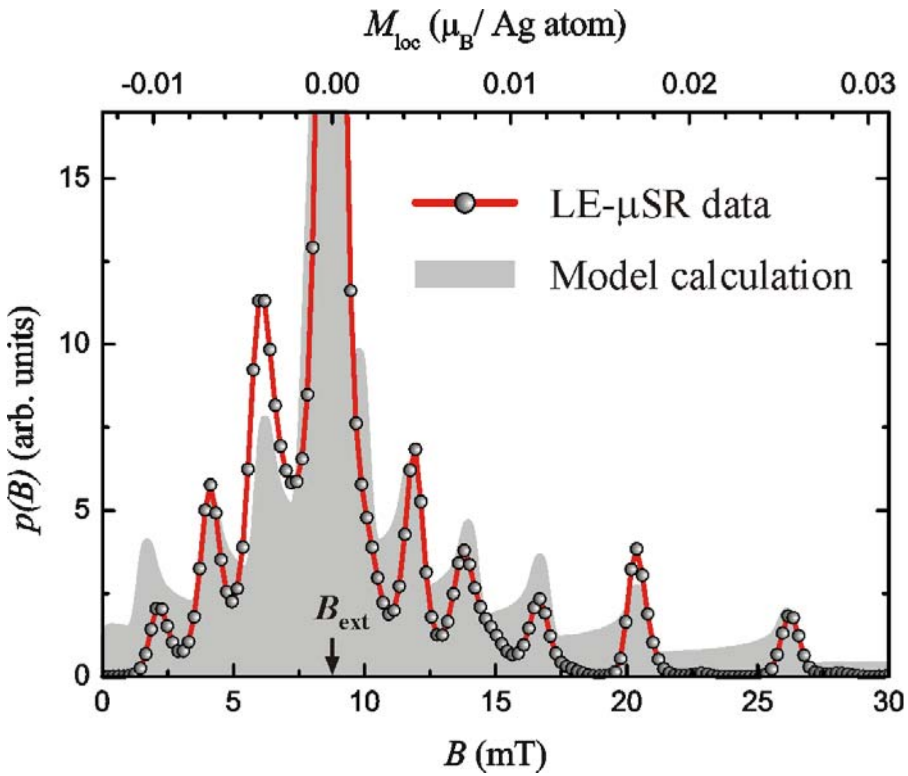

Results:

- P(x) and IEC oscillate with the same period

Attenuation of electron spin polarization: $P(x) \propto \frac{1}{x^{0.8}}$

significantly smaller than the one of IEC strength: $J(d) \propto \frac{1}{d^2}$

(beyond RKKY: quantum well model)

$$J(d) \propto \sum_{i=1}^{2} A_i \frac{1}{d^2} \sin(q_\perp^i d + \theta_i)$$

$$P(x) = \sum_{i=1}^{2} C_i \frac{1}{x^{n_i}} \sin(q_\perp^i x + \theta_i)$$

H. Luetkens et al. Phys Rev. Lett. **91**, 017204 (2003).

Spin Coherent Transport in Organic Spin Valves

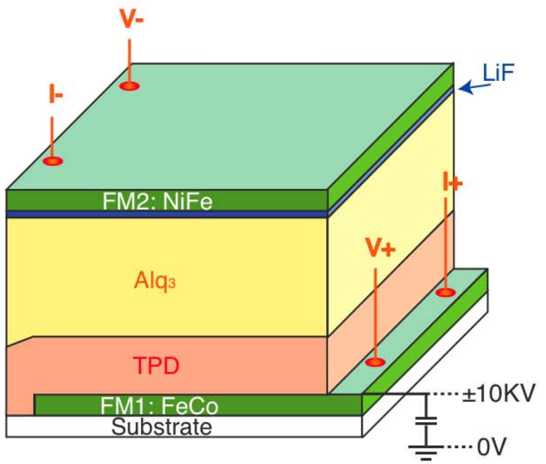

Spacer:

organic semiconductor

Alq3: $C_{27} H_{18} N_3 O_3Al$

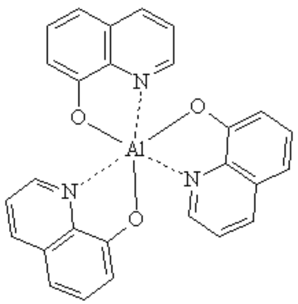

MR vs spacer thickness

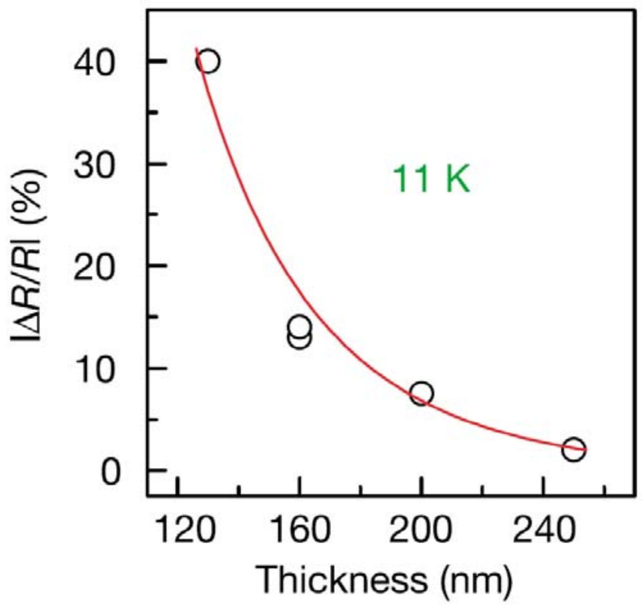

$$MR = \frac{\Delta R}{R} = \frac{R_{AP} - R_P}{R_{AP}}$$

Magnetoresistance vs T

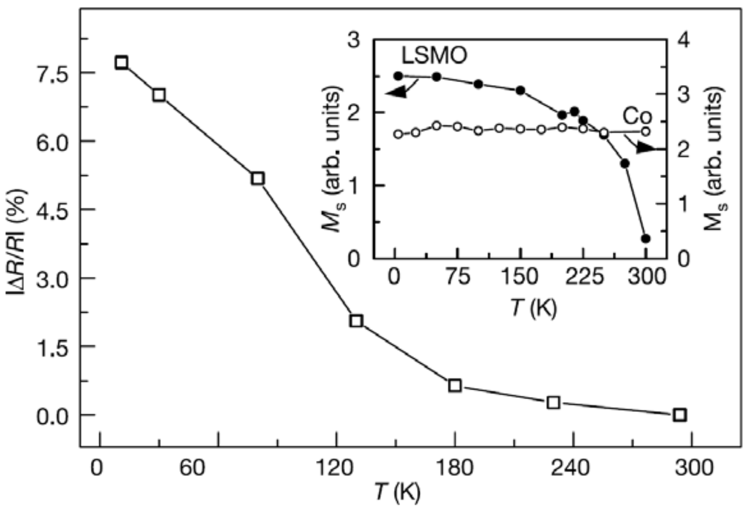

Z.H. Xiong et al.,Nature **427**, 821 (2004)

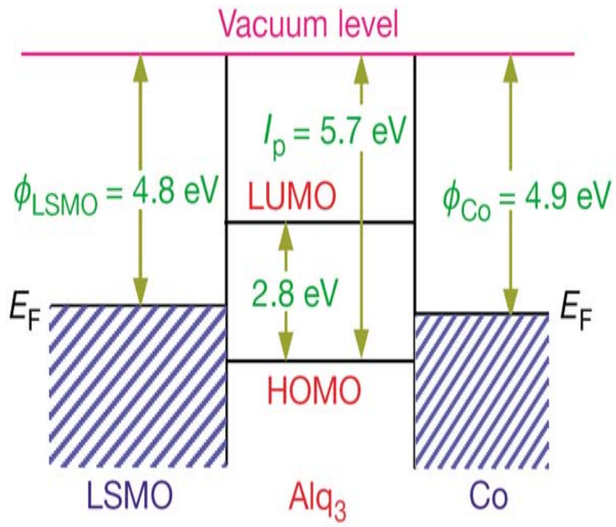

Spin Coherent Transport in Organic Spin Valves

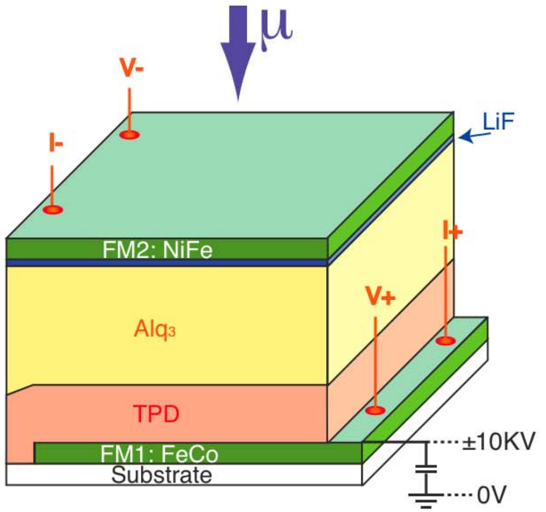

Magnetoresistance vs B

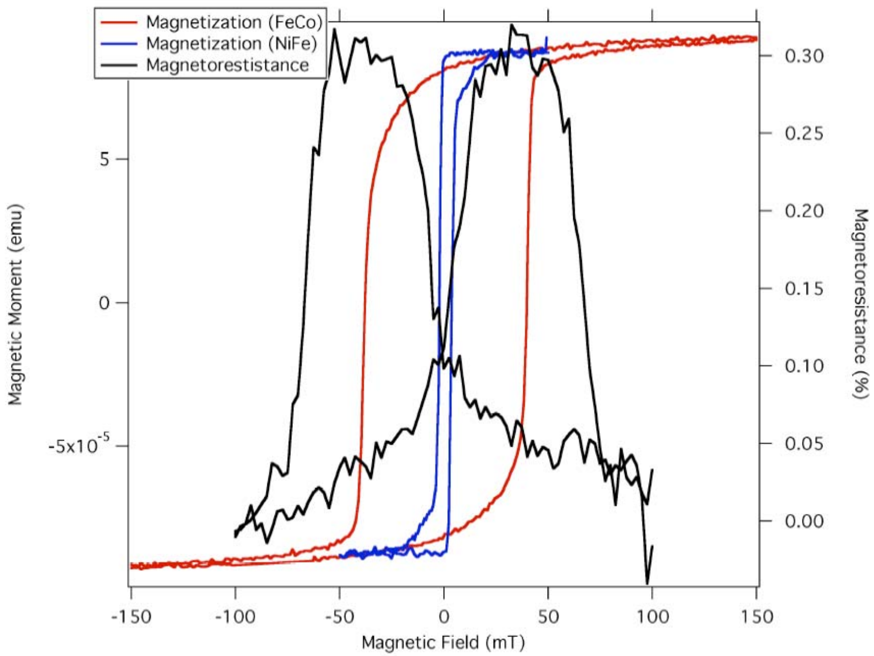

Spacer:

organic semiconductor

Alq3: $C_{27}H_{18}N_3O_3Al$

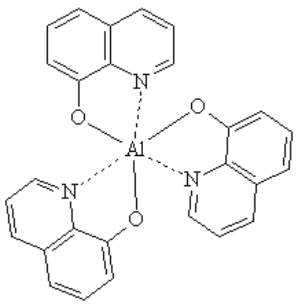

X-rays, n-reflectivity, AFM → very good structural quality, sharp layers and interfaces (rms < 0.5nm)

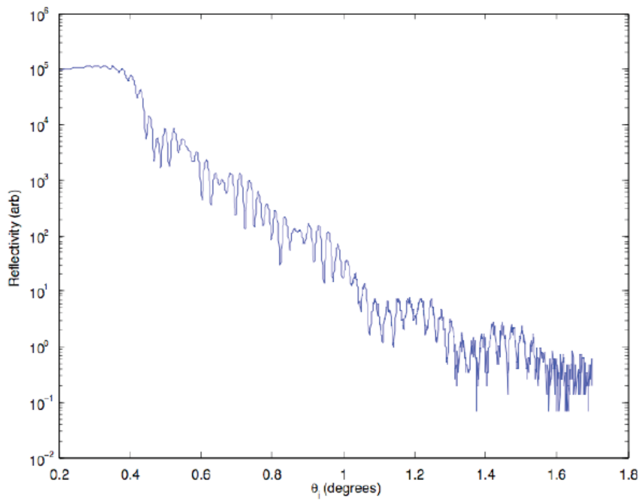

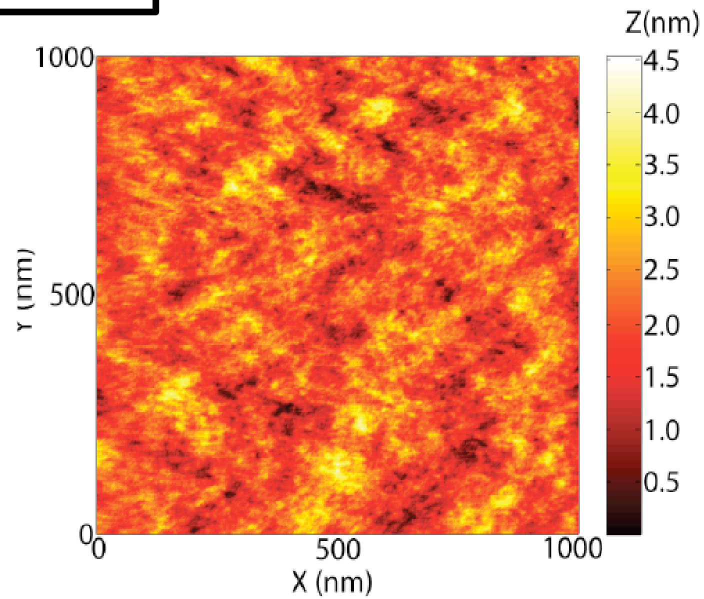

A. J. Drew, J. Hoppler, L. Schulz, F. L. Pratt, P. Desai, P. Shakya, T. Kreouzis, W. P. Gillin, A. Suter, N. A. Morley, V. K. Malik, H. Bouyanfif, K. Kim, A. Dubroka, F. Bourqui, C. Bernhard, R. Scheuermann, T. Prokscha, G. Nieuwenhuys, E. Morenzoni, Nature Materials **8**, 109-114 (2009)

Spin diffusion length in organic spin valve

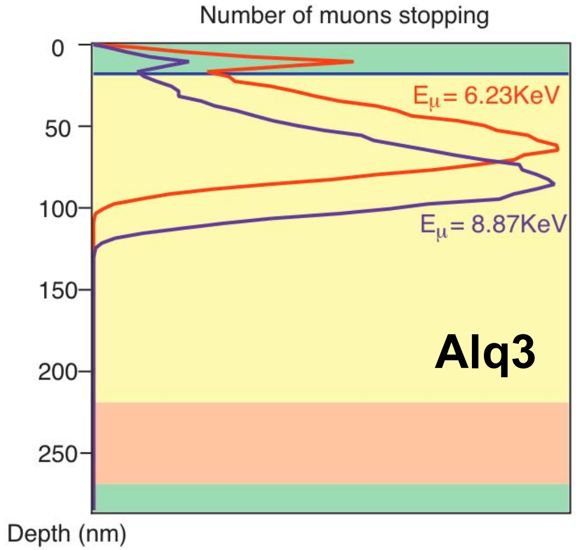

Long coherence time of injected spins ~10^{-5} s → measurable static field.

Field distribution: $I_{on} - I_{off}$

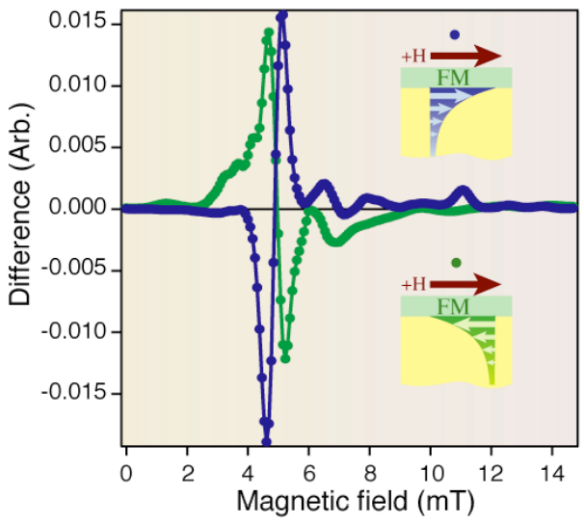

Magnetoresistance vs B

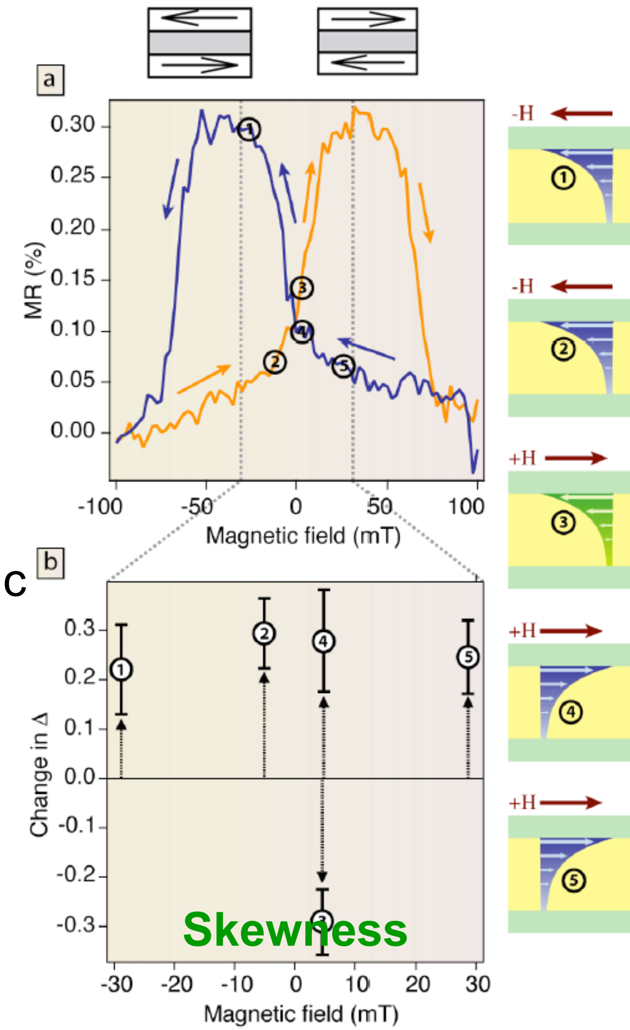

Spin diffusion length vs T correlates with Magnetoresistance

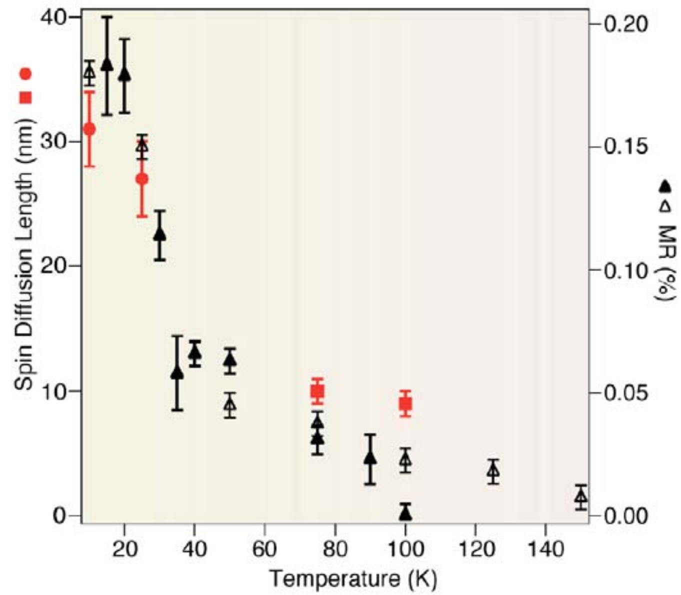

First direct measurement of spin diffusion length in a working spin valve.

A. Drew et al. Nature Materials **8**, 109-114 (2009)